Collective modes: past, present and future perspectives

Muhsin N. Harakeh

KVI, Groningen; GANIL, Caen

International Symposium on *High-resolution Spectroscopy and Tensor interactions* (HST15)

Osaka, Japan

16-19 November 2015

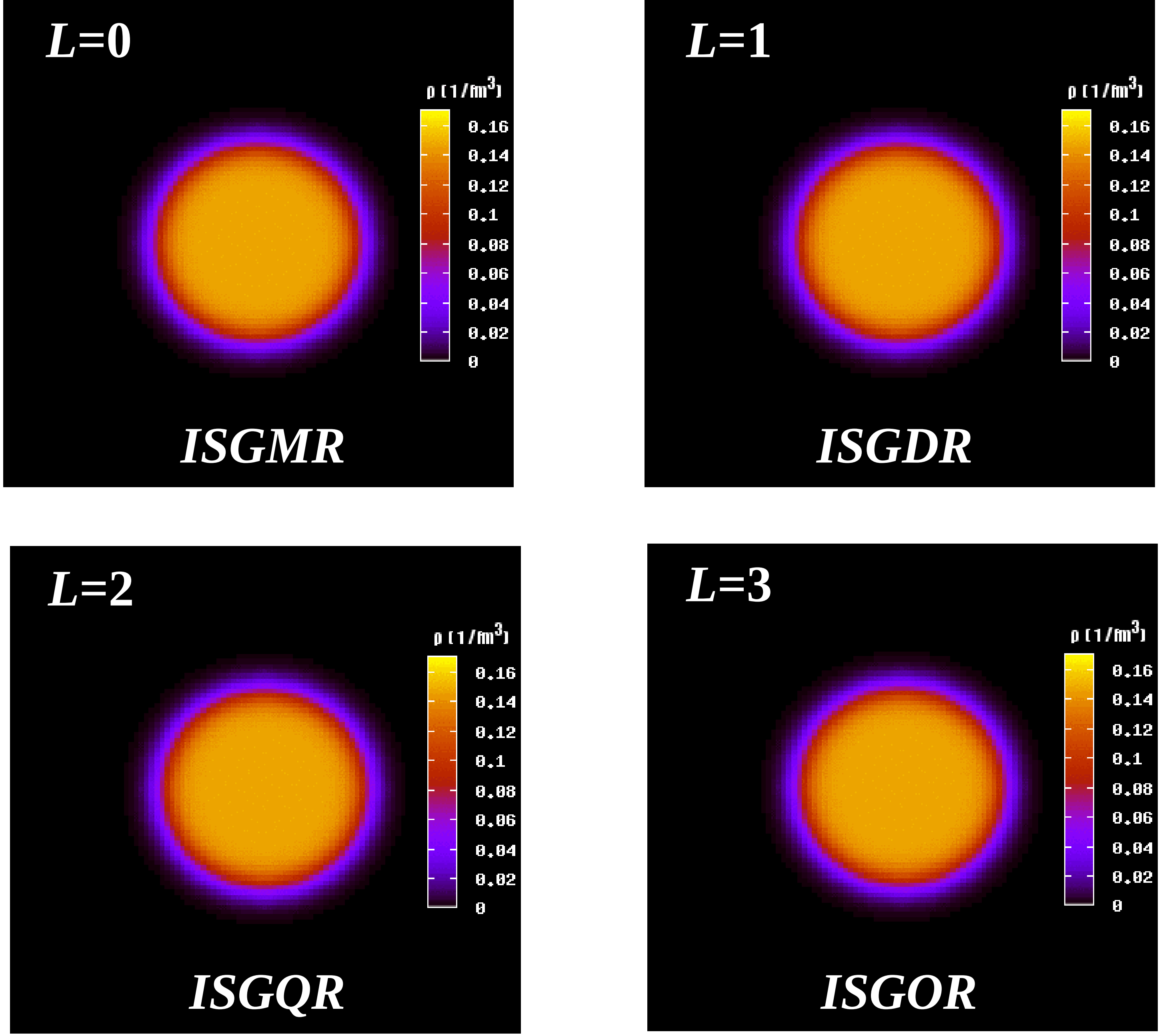
L=0
ρ (1/fm3)
0.16
0.14
0.12
0.1
0.08
0.06
0.04
0.02
0
ISGMR
L=1
ρ (1/fm3)
0.16
0.14
0.12
0.1
0.08
0.06
0.04
0.02
0
ISGDR
L=2
ρ (1/fm3)
0.16
0.14
0.12
0.1
0.08
0.06
0.04
0.02
0
ISGQR
L=3
ρ (1/fm3)
0.16
0.14
0.12
0.1
0.08
0.06
0.04
0.02
0
ISGOR

M. Itoh

Microscopic picture: GRs are coherent (1p-1h) excitations induced by single-particle operators

Microscopic structure of ISGMR & ISGDR

Transition operators:

$$O^{L=0} = \sum_i r_i^0 Y_0^0 + \frac{1}{2}\sum_i r_i^2 Y_0^0 + \ \ldots$$

Constant   Overtone

2ħω excitation

$$O^{L=1} = \sum_i r_i^1 Y_0^1 + \frac{1}{2}\sum_i r_i^3 Y_0^1 + \ \ldots$$

Spurious c.o.m. motion   Overtone

3ħω excitation (overtone of c.o.m. motion)

IVGDR

$\tau r Y_1$

$\Delta N = 1$ **E1 (IVGDR)**

$\Delta N = 2$ **E2 (ISGQR)**

&

$\Delta N = 0$ **E0 (ISGMR)**

ISGMR $r^2 Y_0$

ISGQR $r^2 Y_2$

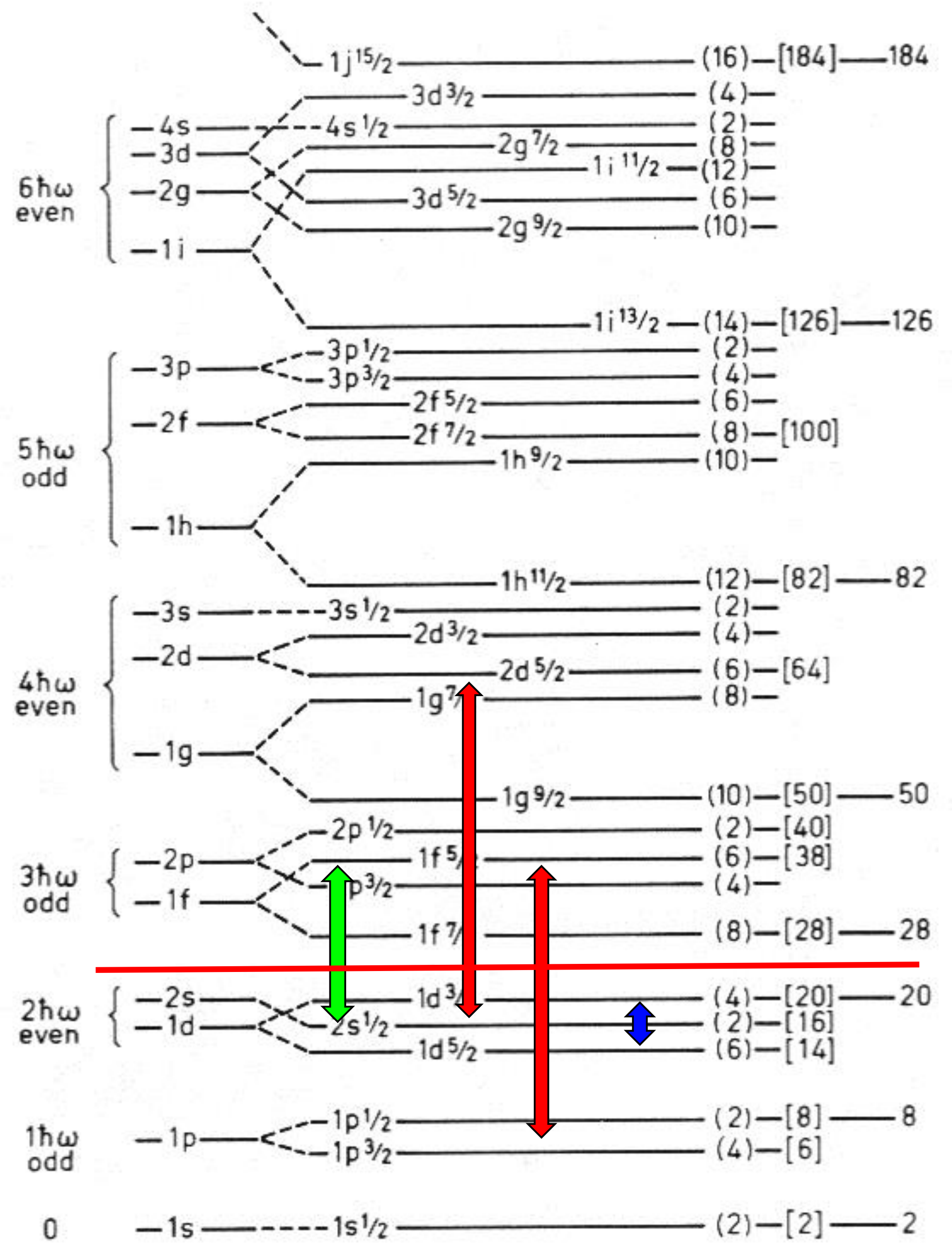

Equation of state (EOS) of nuclear matter

More complex than for infinite neutral liquids
Neutrons and protons with different interactions
Coulomb interaction of protons

1. **Governs the collapse and explosion of giant stars (supernovae)**
2. **Governs formation of neutron stars (mass, radius, crust)**
3. **Governs collisions of heavy ions.**
4. **Important ingredient in the study of nuclear properties.**

For the equation of state of symmetric nuclear matter at saturation nuclear density:

$$\left[\frac{d(E/A)}{d\rho}\right]_{\rho=\rho_0} = 0$$

and one can derive the incompressibility of nuclear matter:

$$K_{nm} = \left[9\rho^2 \frac{d^2(E/A)}{d\rho^2}\right]_{\rho=\rho_0}$$

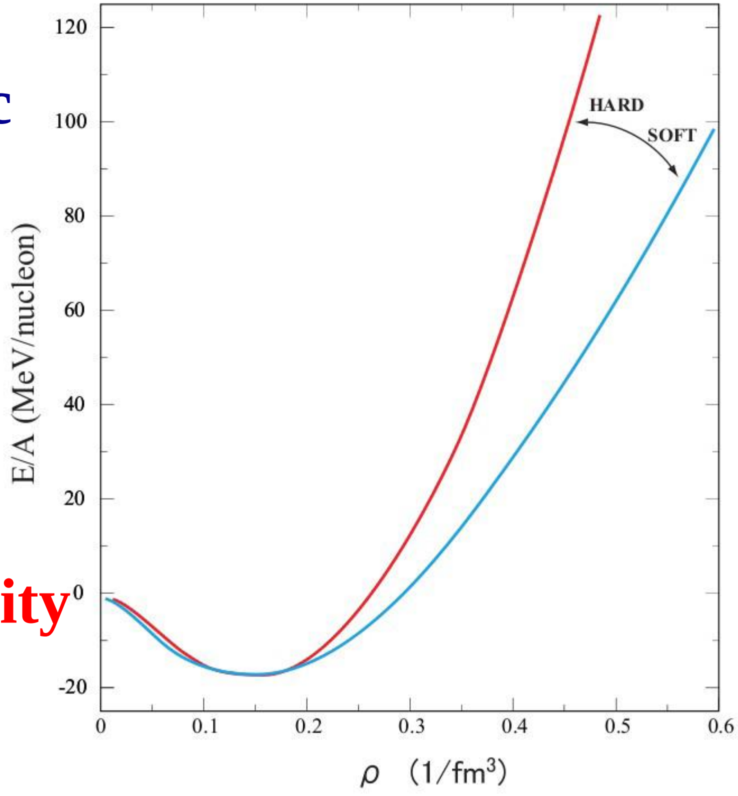

***E/A*: binding energy per nucleon**

***ρ*   : nuclear density**

***ρ₀*   : nuclear density at saturation**

J.P. Blaizot, Phys. Rep. 64, 171 (1980)

Isoscalar Excitation Modes of Nuclei

Hydrodynamic models/Giant Resonances

Coherent vibrations of nucleonic fluids in a nucleus.

Compression modes: ISGMR, ISGDR

In Constrained and Scaling Models:

$$E_{ISGMR} = \hbar\sqrt{\frac{K_A}{m\langle r^2 \rangle}}$$

$$E_{ISGDR} = \hbar\sqrt{\frac{7}{3}\frac{K_A + \frac{27}{25}\varepsilon_F}{m\langle r^2 \rangle}}$$

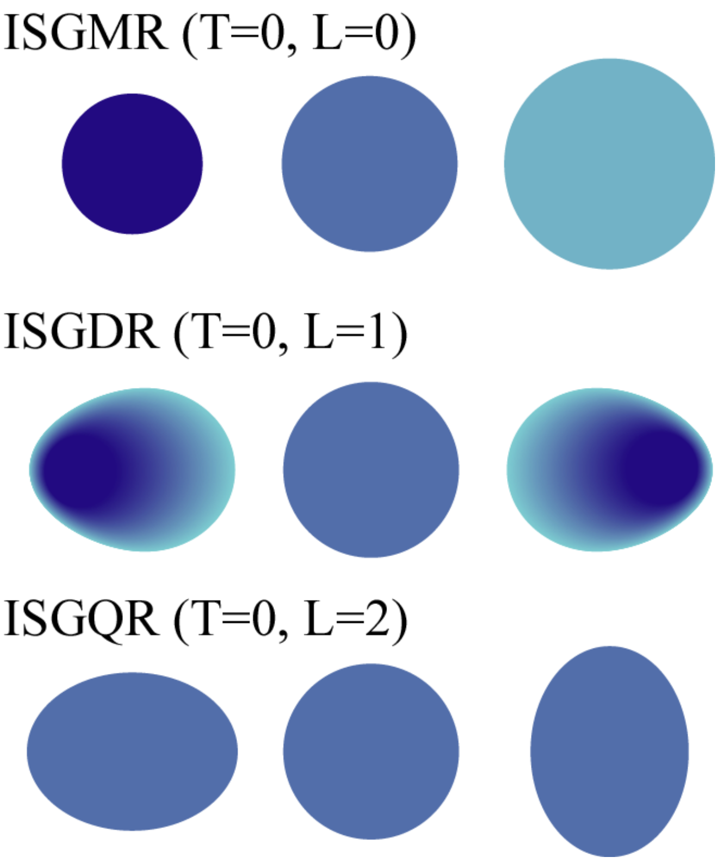

ε_F **is the Fermi energy and the nucleus incompressibility:**

$$\rightarrow \quad K_A = \left[r^2 (d^2(E/A)/dr^2) \right]_{r=R_0}$$

J.P. Blaizot, Phys. Rep. 64 (1980) 171

Giant resonances

- **Macroscopic properties: E_x, Γ, %EWSR**
- **Isoscalar giant resonances; compression modes**

ISGMR, ISGDR ⇒ Incompressibility, symmetry energy

$$K_A = K_{vol} + K_{surf}A^{-1/3} + K_{sym}((N-Z)/A)^2 + K_{Coul}Z^2A^{-4/3}$$

ISGQR, ISGMR

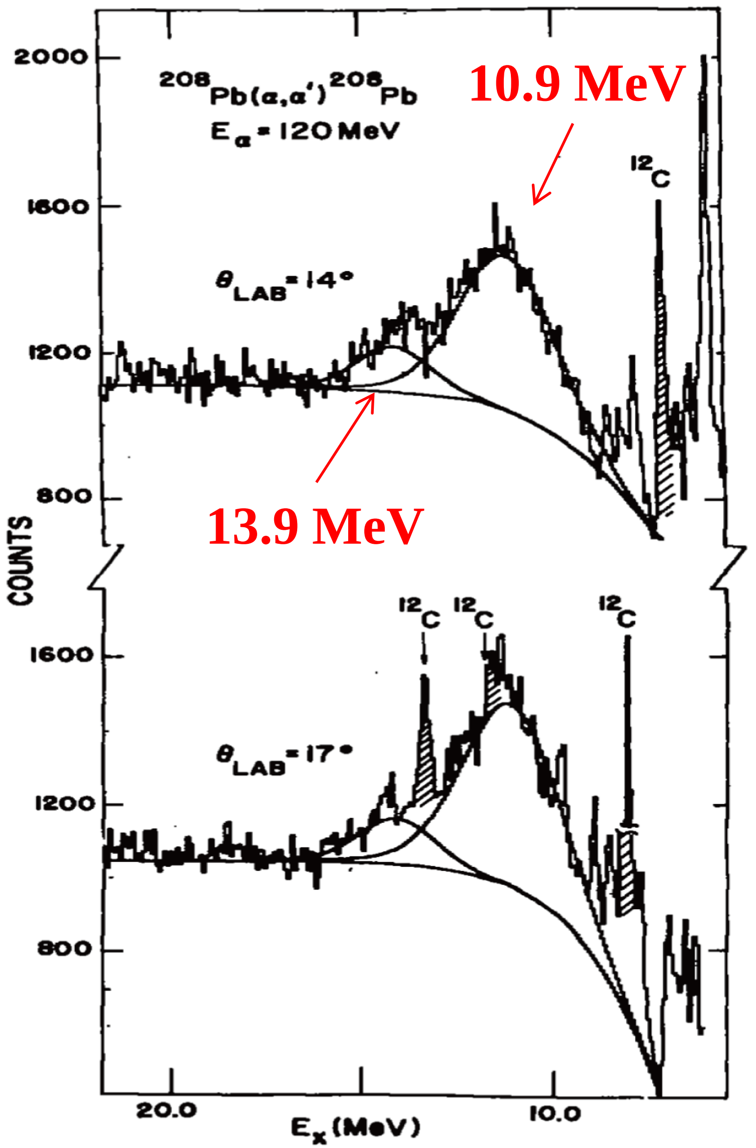

⇐ ^{208}Pb(α,α′) at $E_α$=120 MeV

Large instrumental background and nuclear continuum!

M. N. Harakeh *et al.*, Phys. Rev. Lett. 38, 676 (1977)

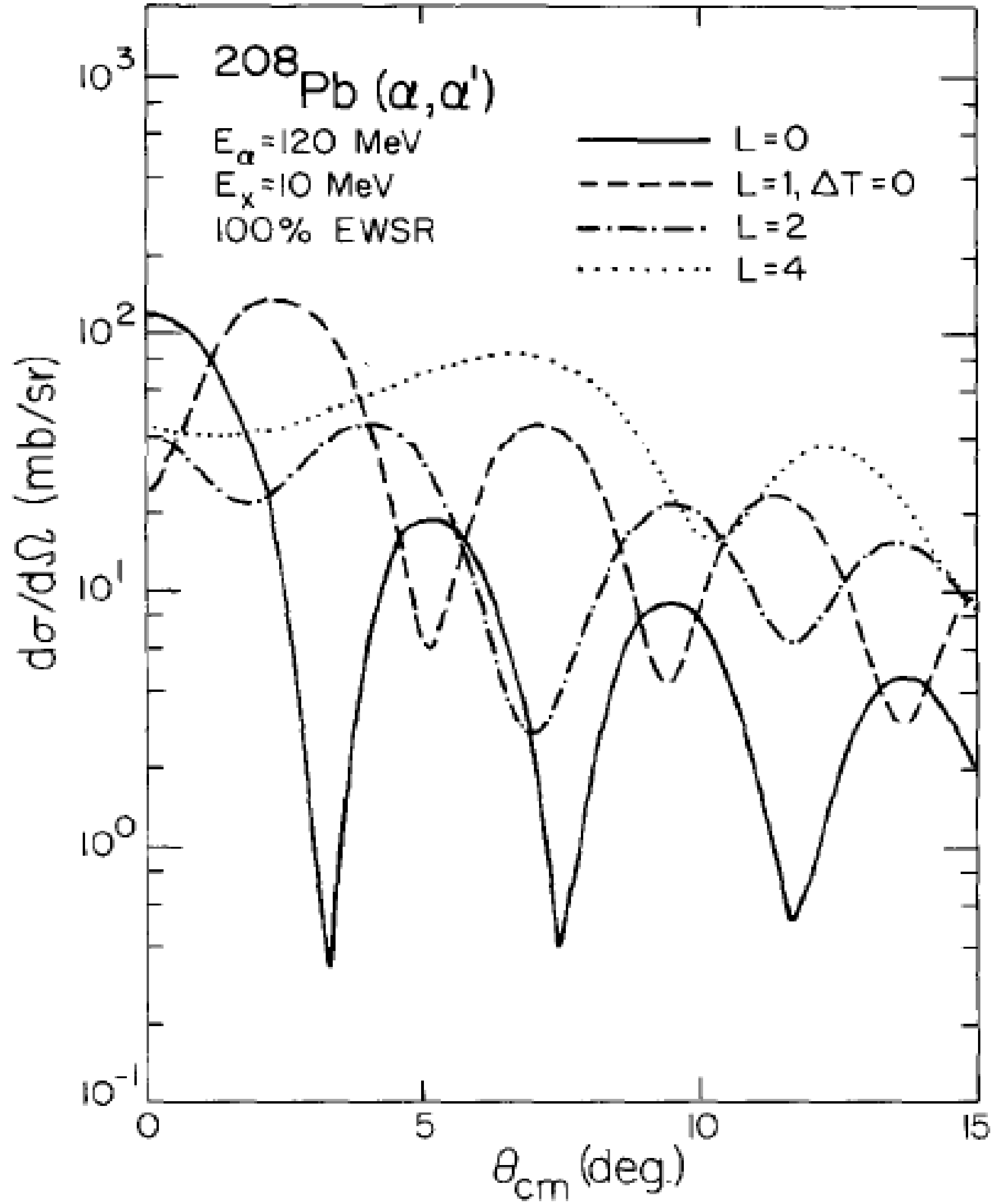

^{208}Pb (α,α')
$E_α$=120 MeV
E_x=10 MeV
100% EWSR
L=0
L=1, ΔT=0
L=2
L=4
10^3
10^2
10^1
10^0
10^{-1}
dσ/dΩ (mb/sr)
0
5
10
15
$θ_{cm}$ (deg.)

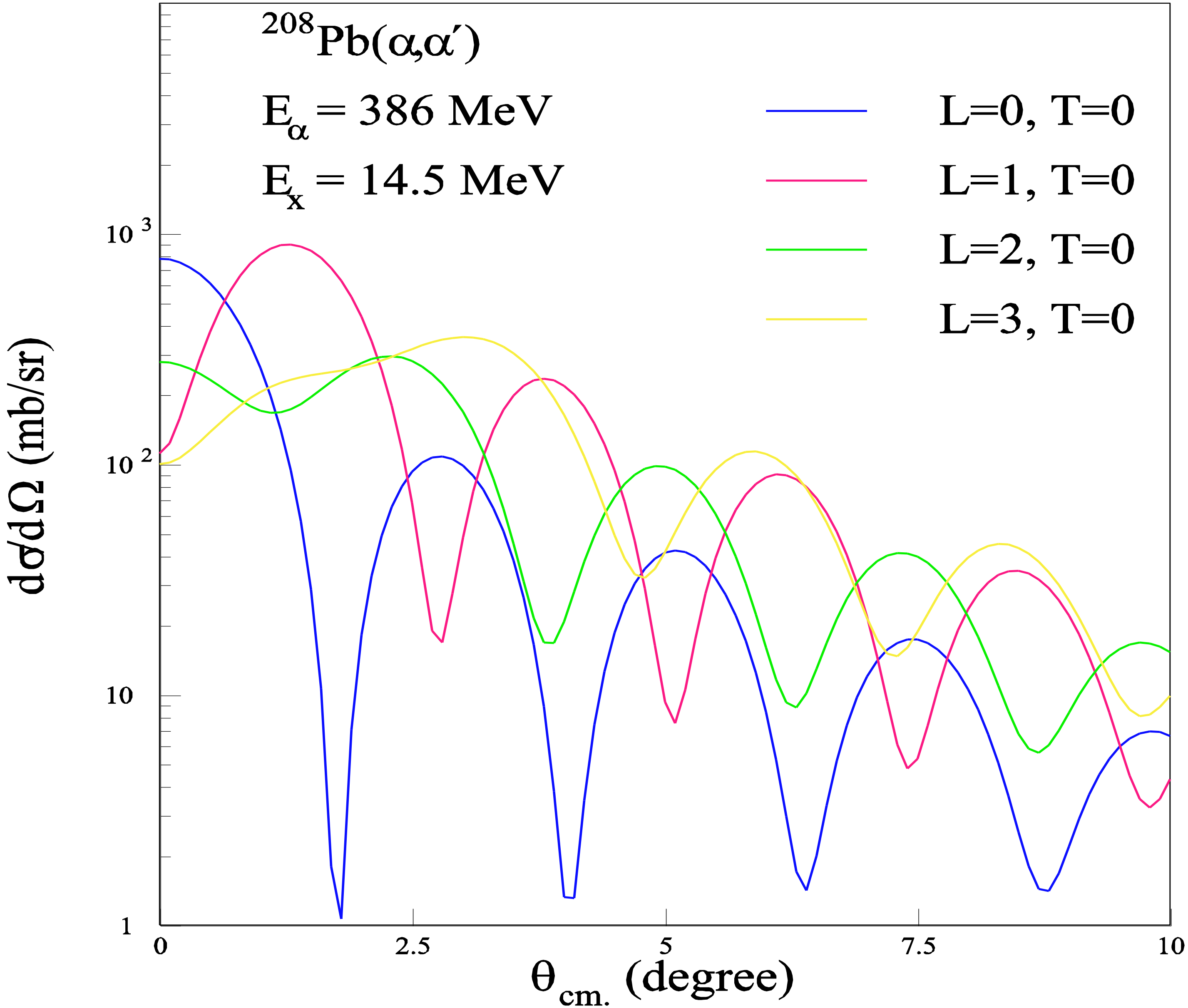

ISGMR, ISGDR

ISGQR, HEOR

100 % EWSR

At E_x= 14.5 MeV

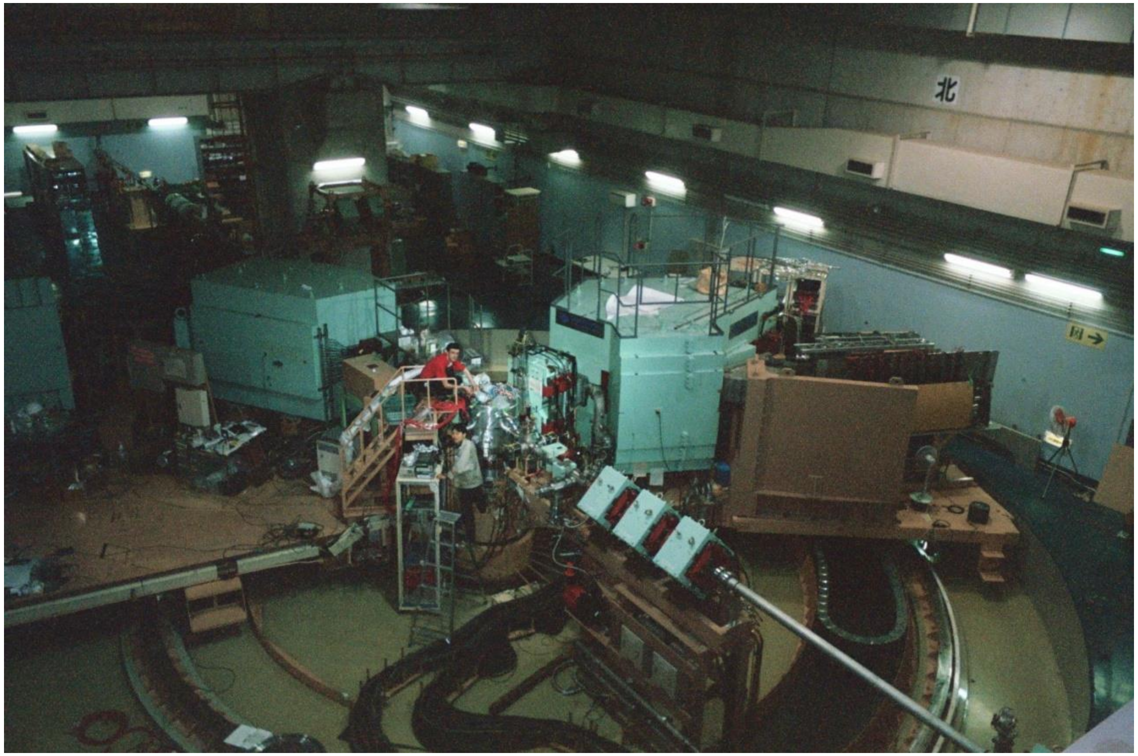

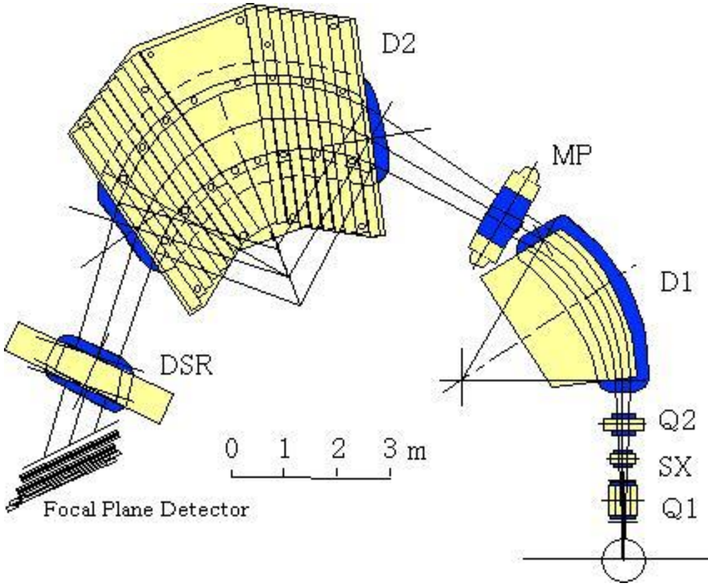

Grand Raiden@ RCNP

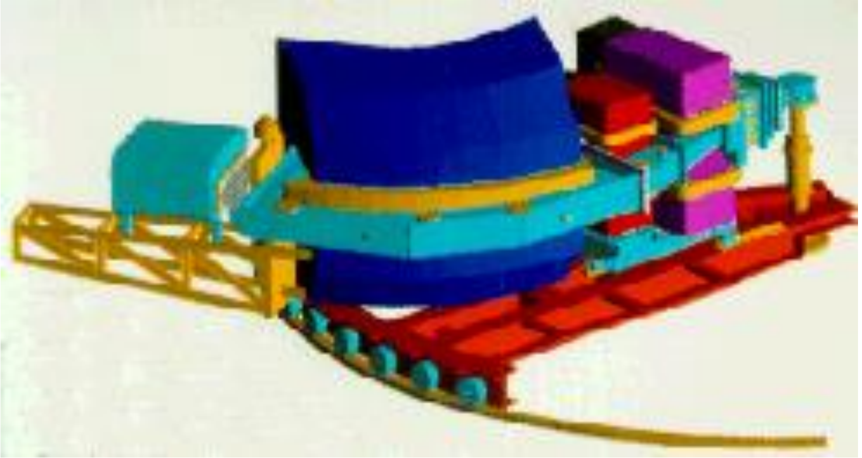

BBS@KVI

(α,α') at E_α~ 400 & 200 MeV at RCNP & KVI, respectively

ISGQR at 10.9 MeV

ISGMR at 13.9 MeV

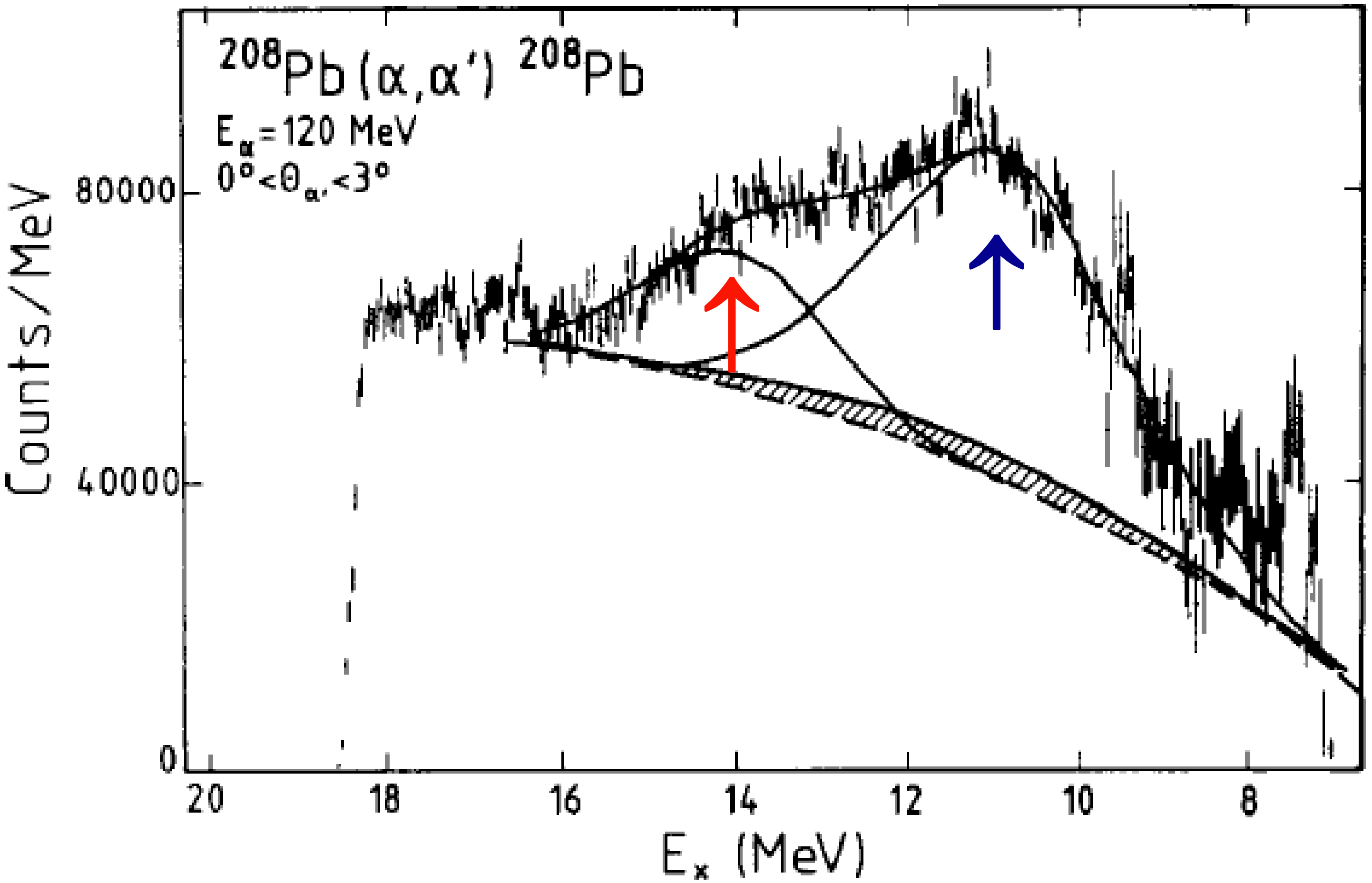

Difference of spectra

$0° < \theta_{\alpha'} < 3°$

$0° < \theta_{\alpha'} < 1.5°$

$1.5° < \theta_{\alpha'} < 3°$

Difference

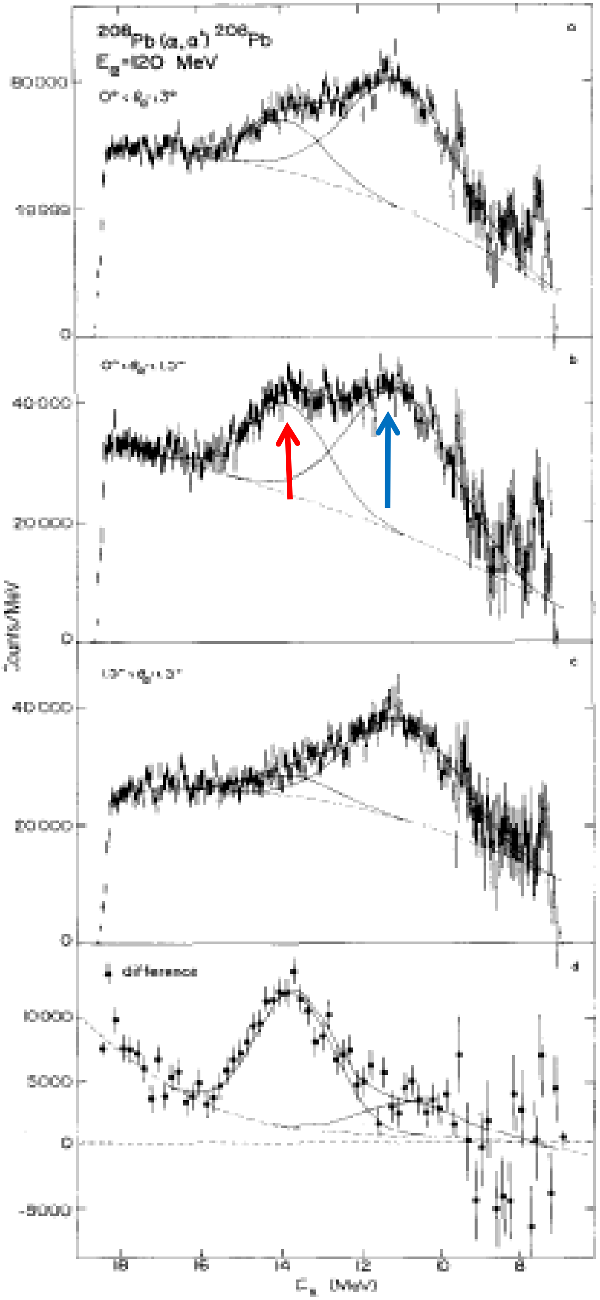

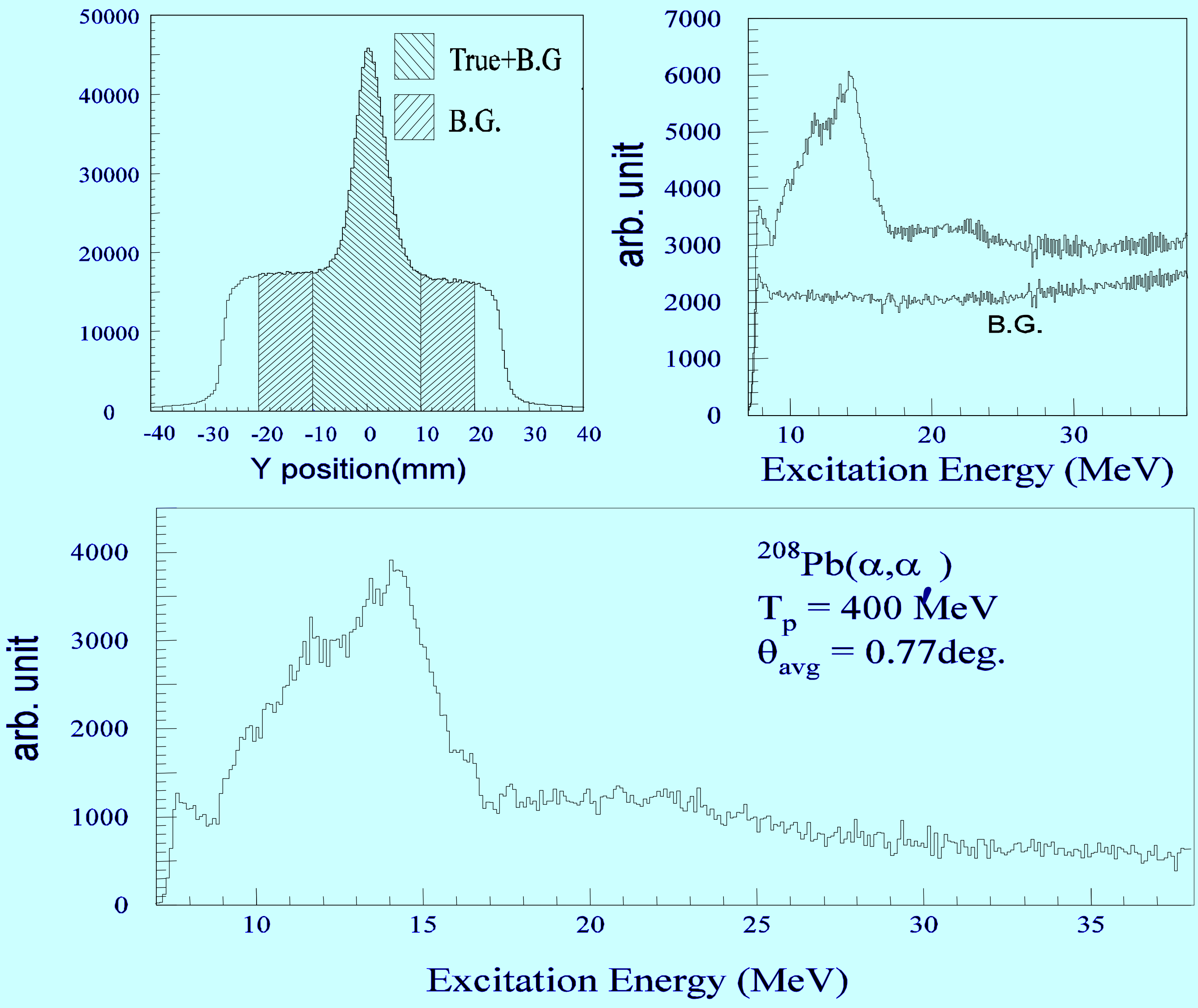
50000
40000
30000
20000
10000
0
-40
-30
-20
-10
0
10
20
30
40
True+B.G
B.G.
Y position(mm)
7000
6000
5000
4000
3000
2000
1000
0
10
20
30
arb. unit
B.G.
Excitation Energy (MeV)
4000
3000
2000
1000
0
10
15
20
25
30
35
arb. unit
^{208}Pb(α,α′)
T_p = 400 MeV
$θ_{avg}$ = 0.77deg.
Excitation Energy (MeV)

Multipole decomposition analysis (MDA)

$$\left(\frac{d^2\sigma}{d\Omega dE}(\vartheta_{c.m.},E)\right)^{\exp.} = \sum_L a_L(E)\left(\frac{d^2\sigma}{d\Omega dE}(\vartheta_{c.m.},E)\right)_L^{calc.}$$

$$\left(\frac{d^2\sigma}{d\Omega dE}(\vartheta_{c.m.},E)\right)^{\exp.} : \text{Experimental cross section}$$

$$\left(\frac{d^2\sigma}{d\Omega dE}(\vartheta_{c.m.},E)\right)_L^{calc.} : \text{DWBA cross section (unit cross section)}$$

$$a_L(E) : \text{EWSR fraction}$$

a. ISGR (L<15)+ IVGDR (through Coulomb excitation)

b. DWBA formalism; single folding ⇒ transition potential

$$\delta U_L(r,E) = \int d\vec{r}'\,\delta\rho_L(\vec{r}',E)[V(|\vec{r}-\vec{r}'|,\rho_0(r')) + \rho_0(r')\frac{\partial V(|\vec{r}-\vec{r}'|,\rho(r'))}{\partial\rho_0(r')}]$$

$$U(r) = \int d\vec{r}'V(|\vec{r}-\vec{r}'|,\rho_0(r'))\rho_0(r')$$

Transition density

- **ISGMR Satchler, Nucl. Phys. A472 (1987) 215**

$$\delta\rho_0(r,E) = -\alpha_0[3 + r\frac{d}{dr}]\rho_0(r)$$

$$\alpha_0^2 = \frac{2\pi\hbar^2}{mA < r^2 > E}$$

- **ISGDR Harakeh & Dieperink, Phys. Rev. C23 (1981) 2329**

$$\delta\rho_1(r,E) = -\frac{\beta_1}{R\sqrt{3}}[3r^2\frac{d}{dr} + 10r - \frac{5}{3} < r^2 > \frac{d}{dr} + \varepsilon(r\frac{d^2}{dr^2} + 4\frac{d}{dr})]\rho_0(r)$$

$$\beta_1^2 = \frac{6\pi\hbar^2}{mAE}\frac{R^2}{(11 < r^4 > -(25/3) < r^2 >^2 - 10\varepsilon < r^2 >)}$$

- **Other modes Bohr-Mottelson (BM) model**

$$\delta\rho_L(r,E) = -\delta_L\frac{d}{dr}\rho_0(r)$$

$$\delta_L^2 = (\beta_L c)^2 = \frac{L(2L+1)^2}{(L+2)^2}\frac{2\pi\hbar^2}{mAE}\frac{< r^{2L-2} >}{< r^{L-1} >^2}$$

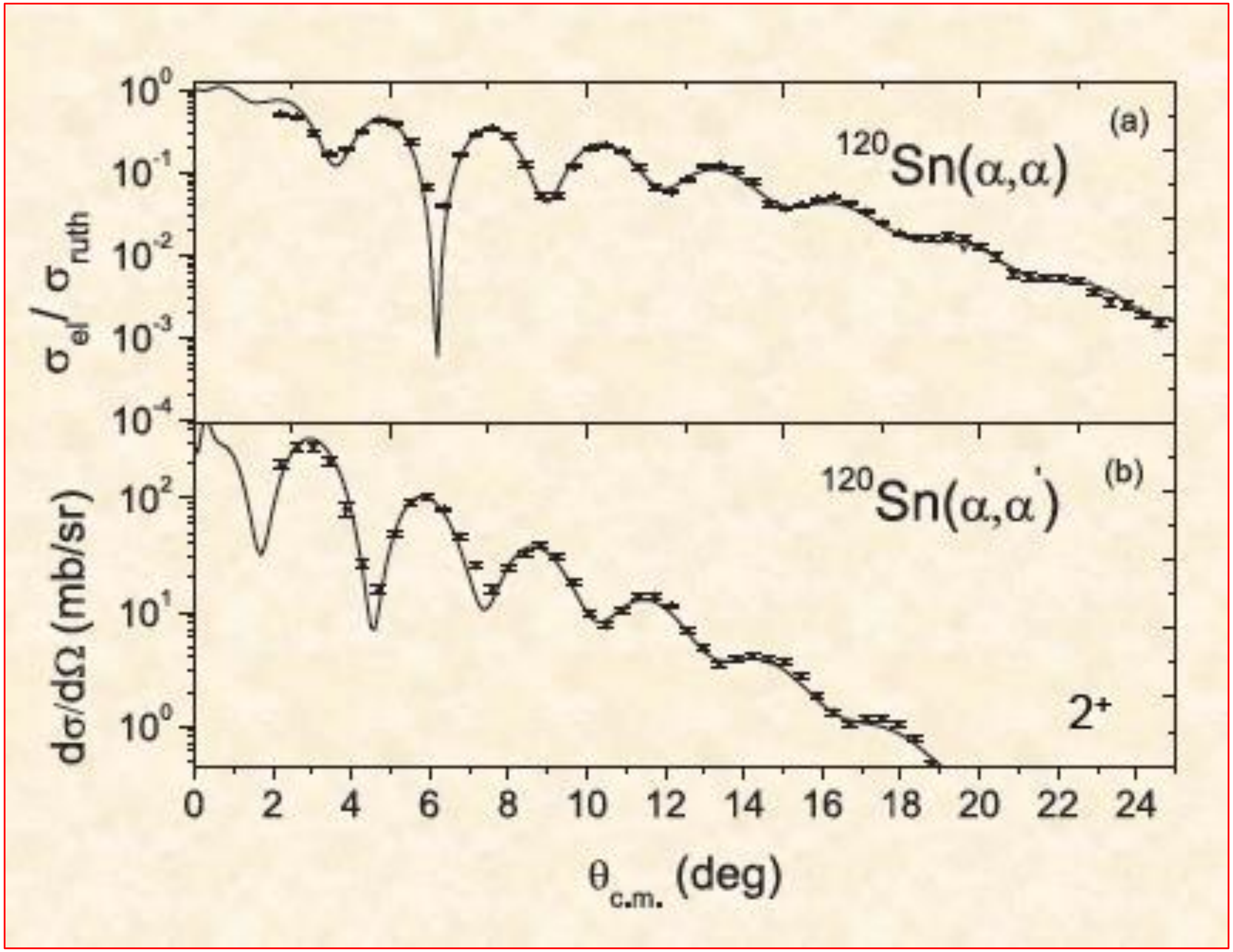

$\sigma_{el}/\sigma_{ruth}$
$^{120}Sn(\alpha,\alpha)$
(a)
$^{120}Sn(\alpha,\alpha')$
(b)
2+
dσ/dΩ (mb/sr)
$\theta_{c.m.}$ (deg)

Uchida *et al.*,
Phys. Lett. B557 (2003) 12
Phys. Rev. C69 (2004) 051301

(α,α′) spectra at 386 MeV

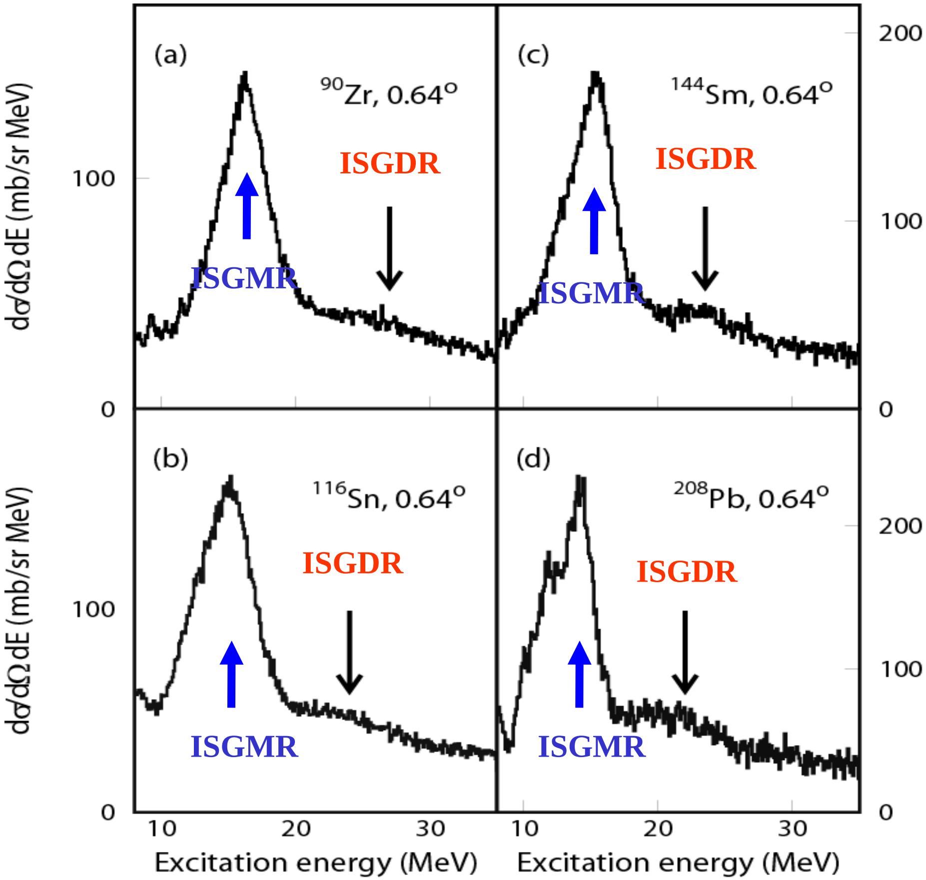

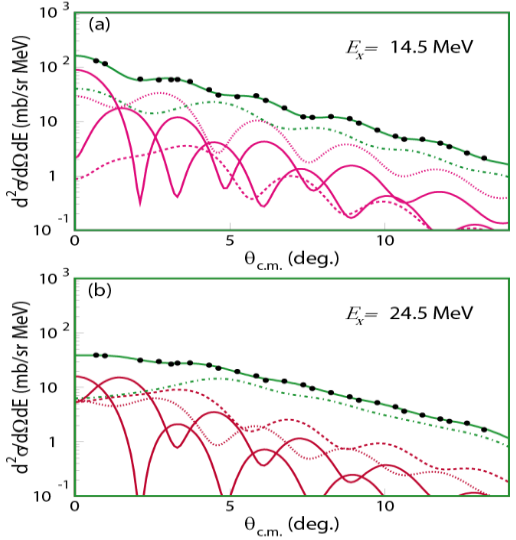

^{116}Sn

MDA results for L=0 and L=1

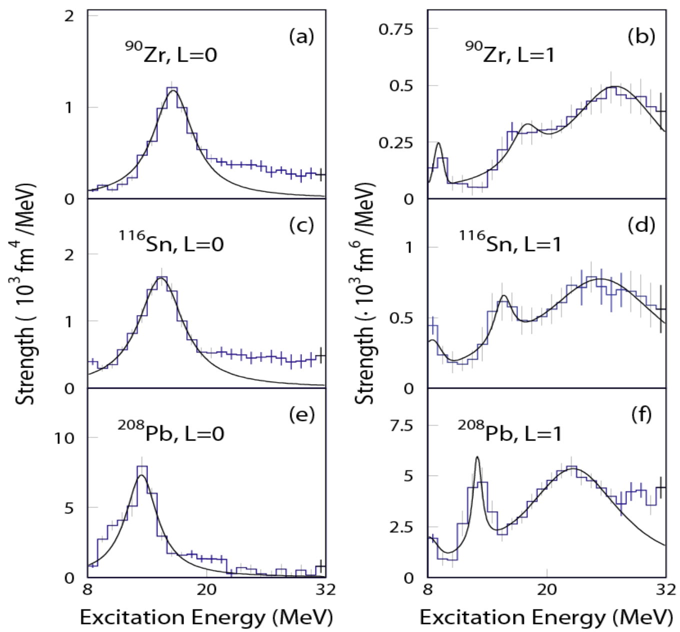

In HF+RPA calculations,

$$K_{nm} = \left[9\rho^2 \frac{d^2(E/A)}{d\rho^2} \right]_{\rho=\rho_0}$$

Nuclear matter

***E/A*: binding energy per nucleon**

***ρ* : nuclear density**

ρ_0 : nuclear density at saturation

K_A: incompressibility

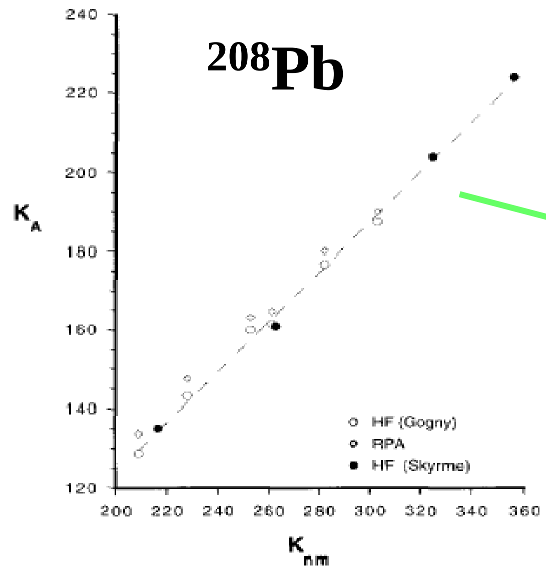

K_A is obtained from excitation energy of ISGMR & ISGDR

$K_A = 0.64K_{nm} - 3.5$

J.P. Blaizot, NPA591, 435 (1995)

From GMR data on ^{208}Pb and ^{90}Zr,

K_∞ = 240 ± 10 MeV [± 20 MeV]

[See, *e.g*., G. Colò *et al*., Phys. Rev. C 70 (2004) 024307]

This number is consistent
with both ISGMR and ISGDR Data
and
with non-relativistic and relativistic calculations

Isoscalar GMR strength distribution in Sn-isotopes obtained by Multipole Decomposition Analysis of singles spectra obtained in ^{A}Sn(α,α′) measurements at incident energy 400 MeV and angles from 0º to 9º

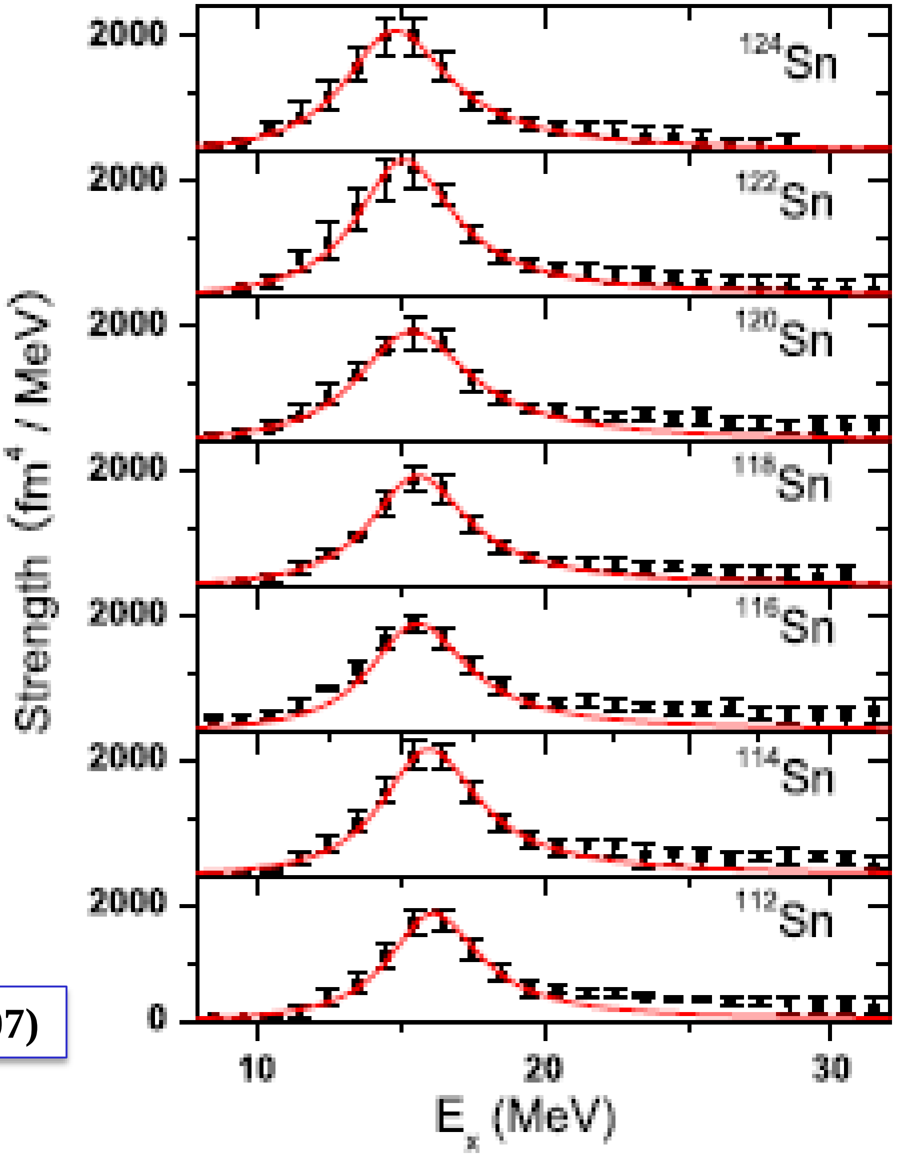

T. Li *et al*., Phys. Rev. Lett. 99, 162503 (2007)

$$K_A = K_{vol} + K_{surf} A^{-1/3} + K_{sym}((N-Z)/A)^2 + K_{coul} Z^2 A^{-4/3}$$

$$K_A \sim K_{vol}(1 + cA^{-1/3}) + K_{\tau}((N - Z)/A)^2 + K_{Coul} Z^2 A^{-4/3}$$

$$K_A - K_{Coul} Z^2 A^{-4/3} \sim K_{vol}(1 + cA^{-1/3}) + K_{\tau}((N - Z)/A)^2$$

$$\sim \text{Constant} + K_{\tau}((N - Z)/A)^2$$

We use K_{Coul} = - 5.2 MeV (from Sagawa)

$(N - Z)/A$

^{112}Sn – ^{124}Sn: 0.107 – 0.194

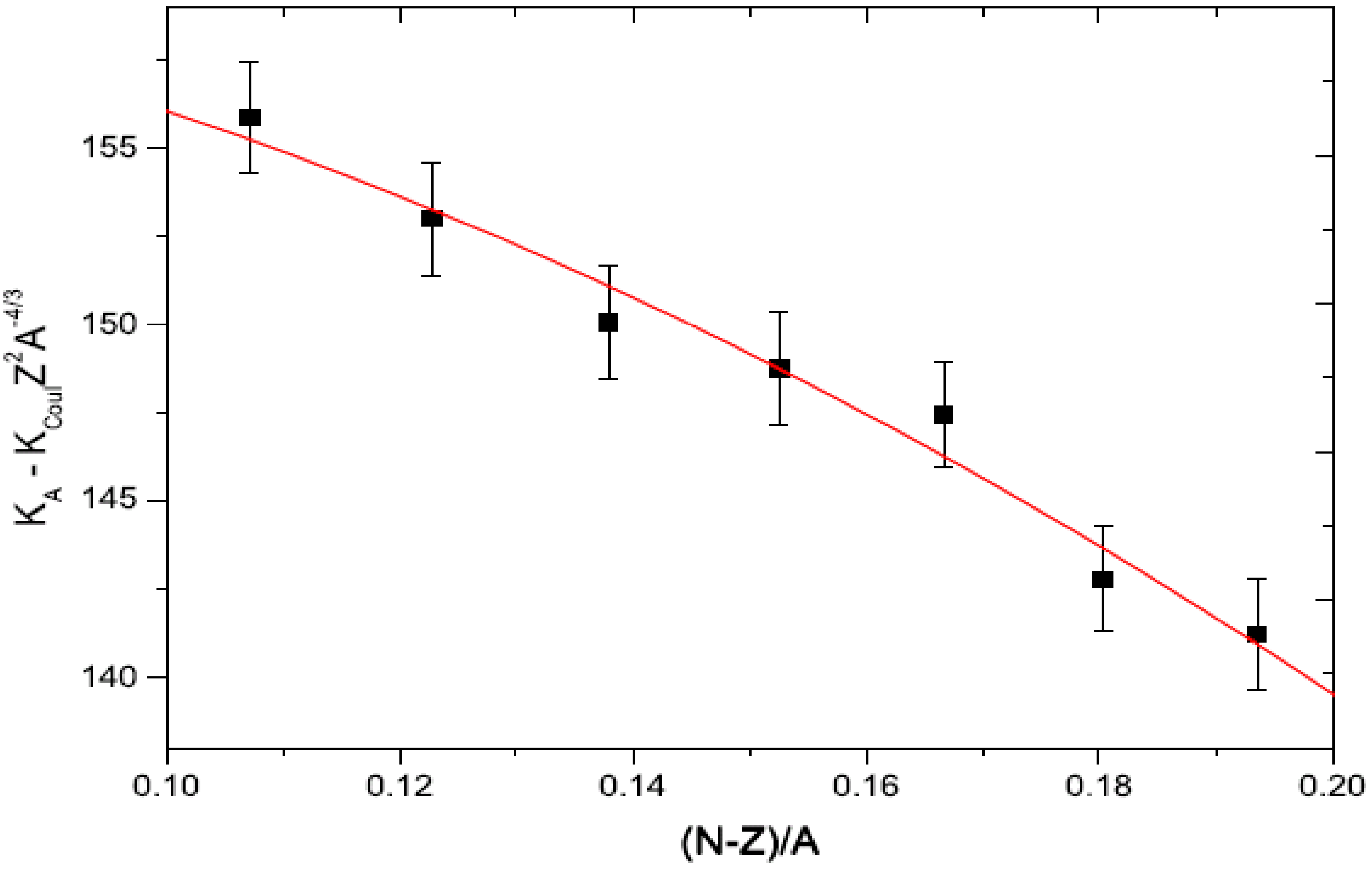

$$K_\tau = -550 \pm 100 \text{ MeV}$$

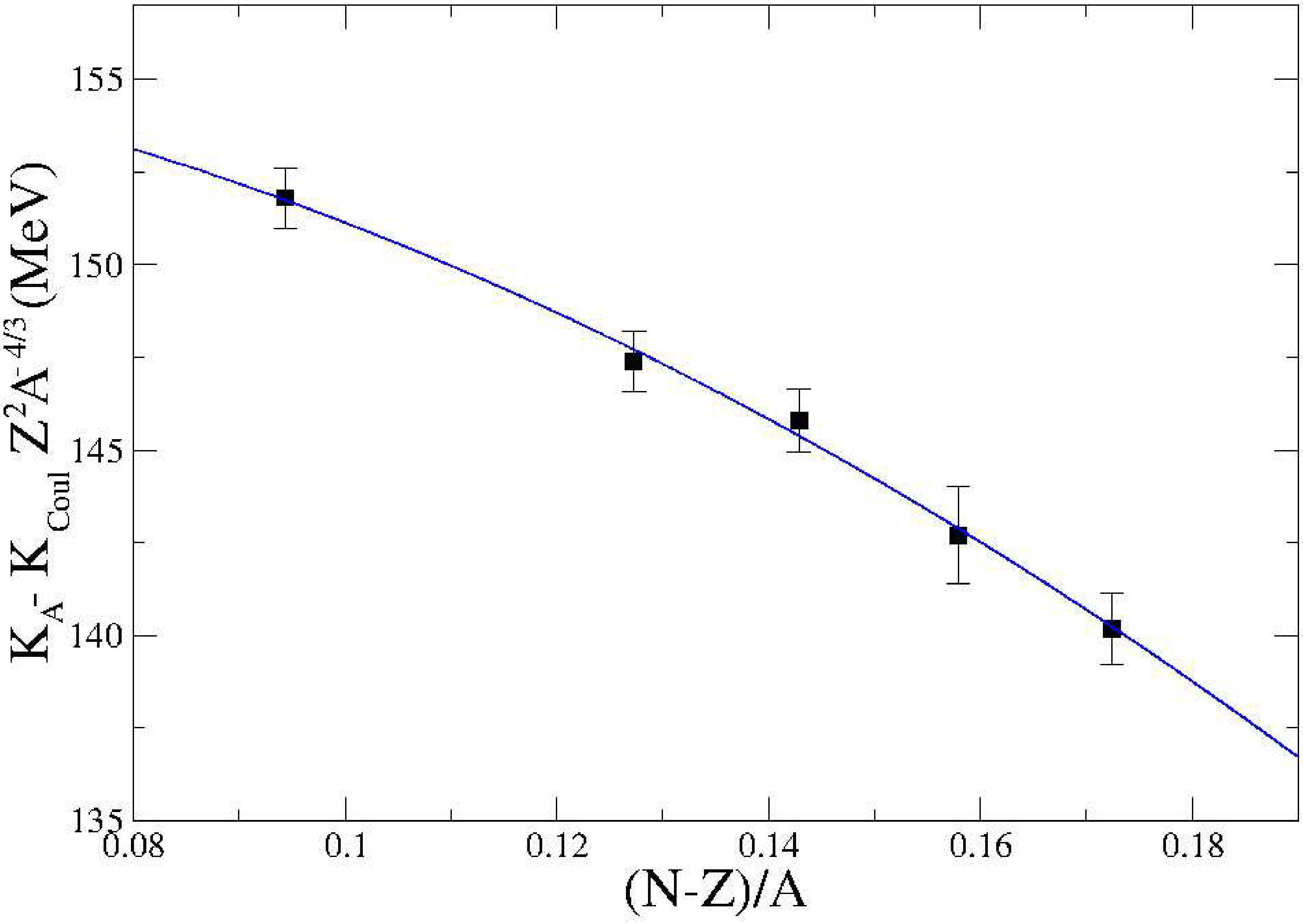

$$K_\tau = -555 \pm 75\,\text{MeV}$$

D. Patel *et al*., Phys. Lett. B 718, 447 (2012)

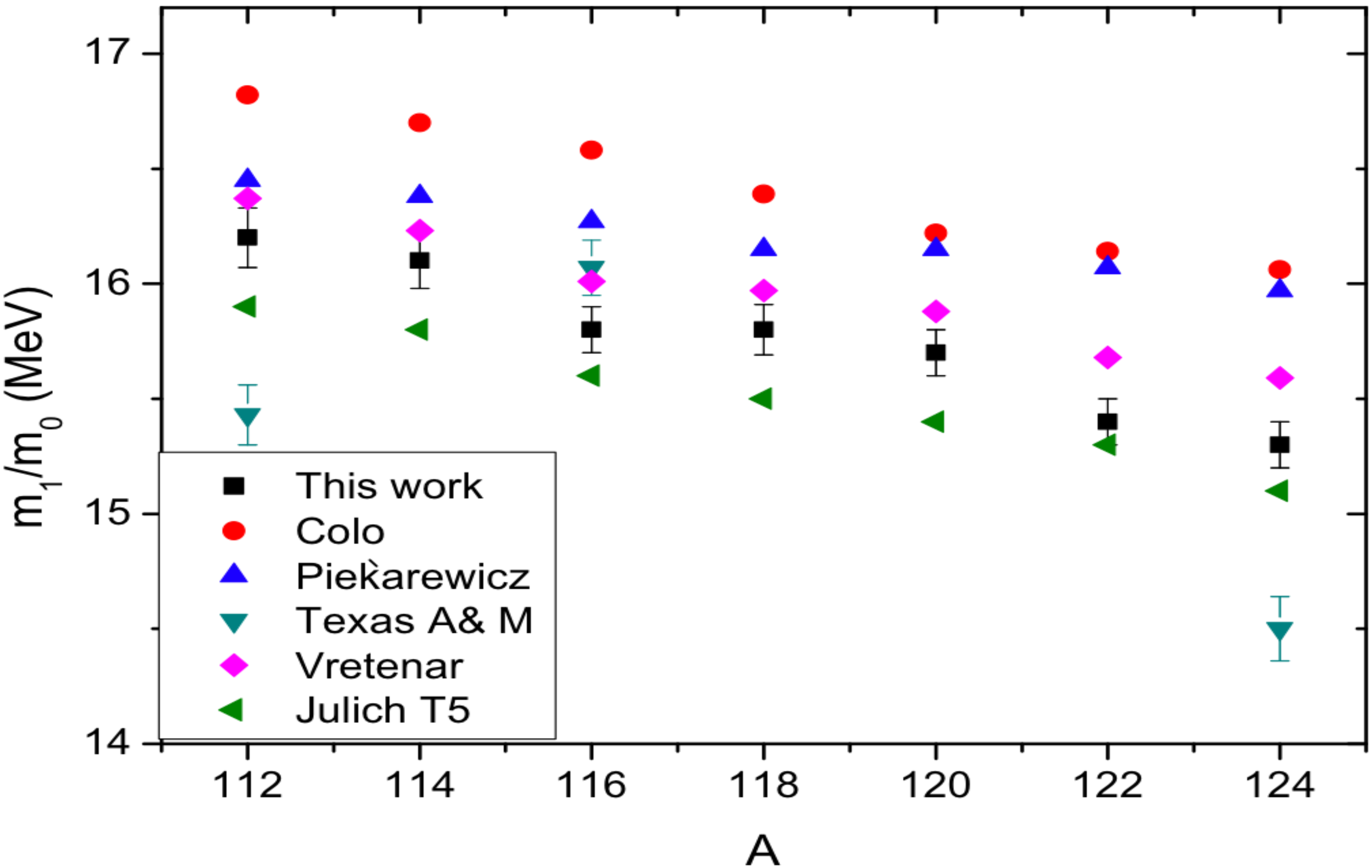

RPA [K_∞ = 240 MeV]; RRPA FSUGold [K_∞ = 230 MeV];
RMF (DD-ME2) [K_∞ = 240 MeV]; (QTBA) (T5 Skyrme) [K_∞ = 202 MeV]

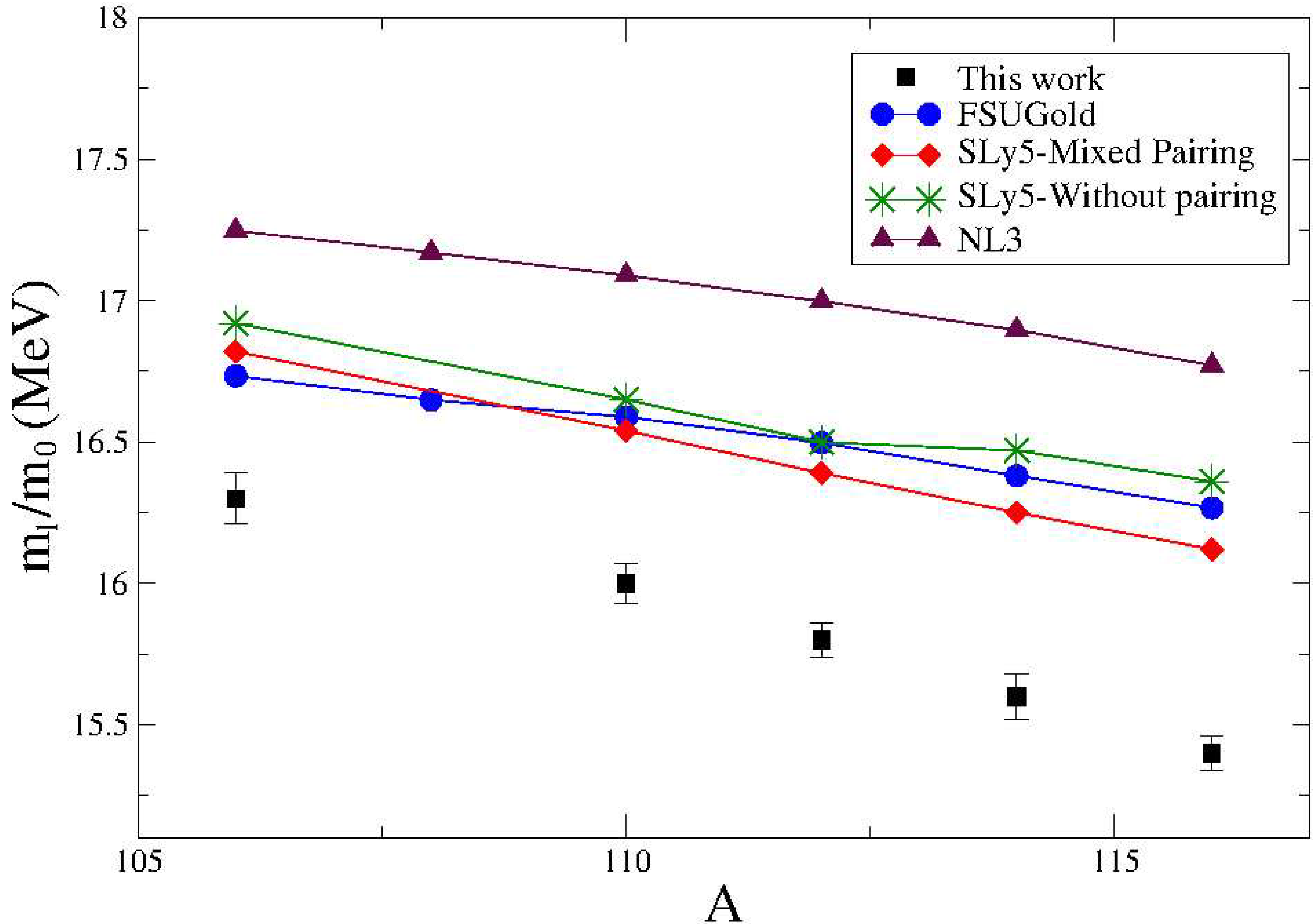

RRPA: FSUGold [K_∞ = 230 MeV]; SLy5 [K_∞ = 230 MeV]; NL3 [K_∞ = 271 MeV]

E. Khan, PRC 80, 011307(R) (2009)

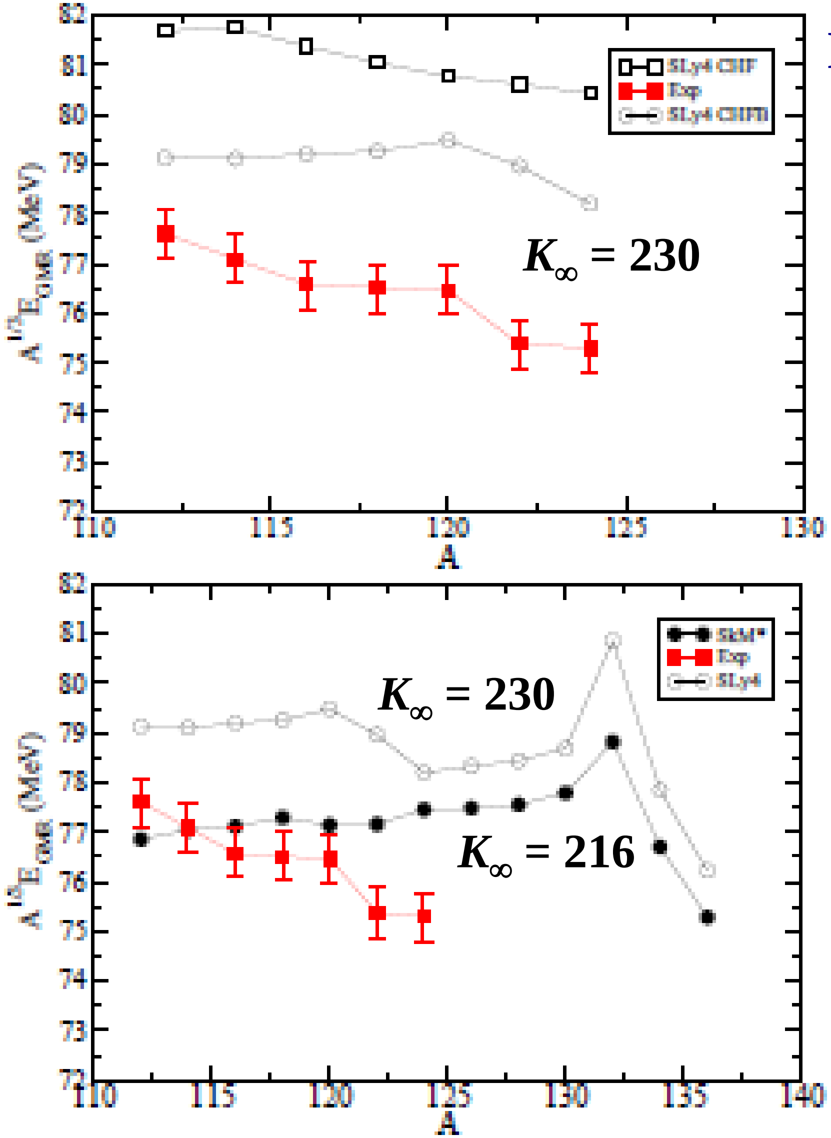

The Giant Monopole Resonances in Pb isotopes

E. Khan, Phys. Rev. C 80, 057302 (2009).

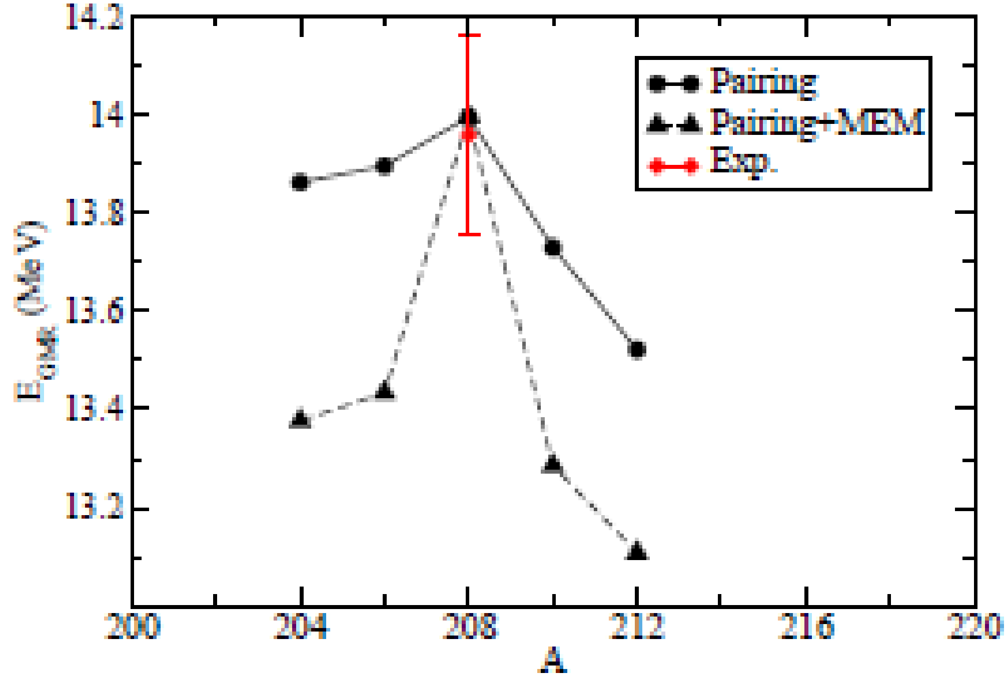

FIG. 2: Excitations energies of the GMR in $^{204-212}$Pb isotopes calculated with constrained HFB method, taking into account the MEM effect (see text). The experimental data is taken from Ref. [22]

Mutually Enhanced Magicity (MEM)?

0^0 spectra

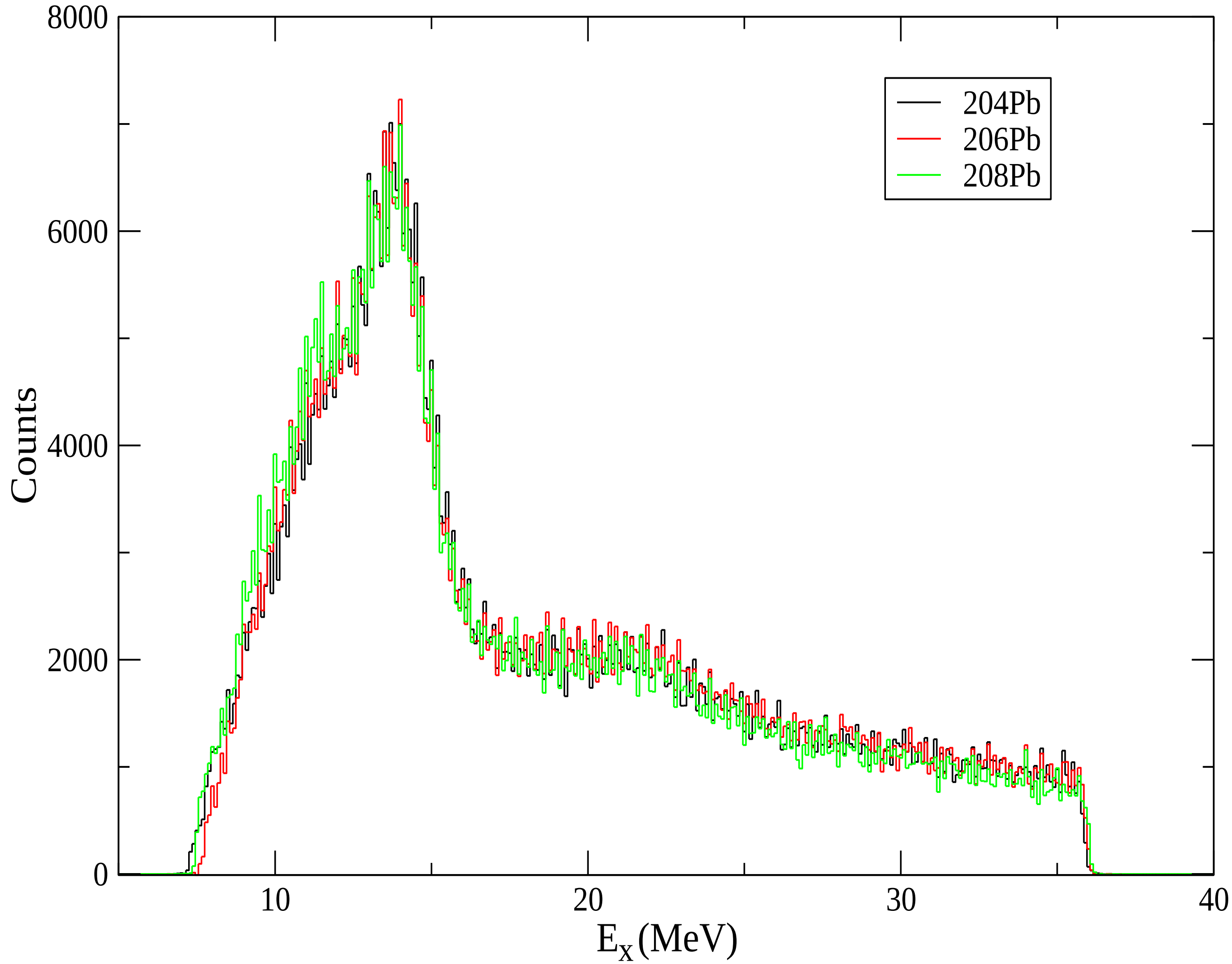

8000
6000
4000
2000
0
Counts
10
20
30
40
E_X(MeV)
204Pb
206Pb
208Pb

Conclusions!

- **There has been much progress in understanding ISGMR & ISGDR macroscopic properties**

Systematics: E_x, Γ, %EWSR

$\Rightarrow K_{nm} \approx$ 240 MeV

$\Rightarrow K_{\tau} \approx -$ 500 MeV

- **Sn and Cd nuclei are softer than ^{208}Pb and ^{90}Zr.**

Challenges with exotic beams

- **Inverse kinematics**

^{56}Ni(α,α′)^{56}Ni*
α = Target
^{56}Ni = Projectile

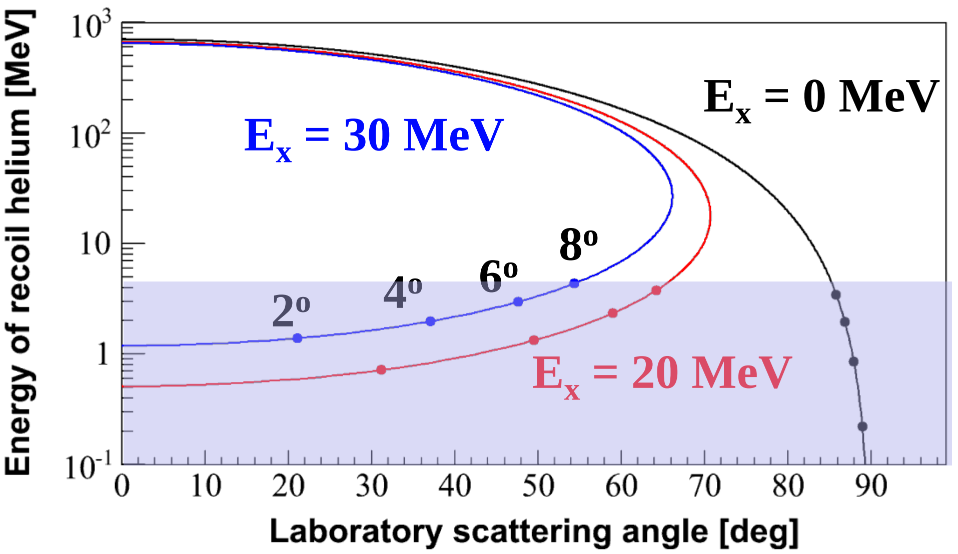

- **Intensity of exotic beams is very low (~10^4 – 10^5 pps)**
- **To get reasonable yields thick target is needed**
- **Very low energy (~ sub MeV) recoil particle will not come out of the thick target**

Nuclear structure studies with reactions in inverse kinematics

- Possible at FAIR, RIKEN, GANIL, FRIB

(beam energies of 50-100 MeV/u are needed!)

Approach at GSI-FAIR (EXL):
Helium gas-jet target
Measure the recoiling alphas

(α,α′)

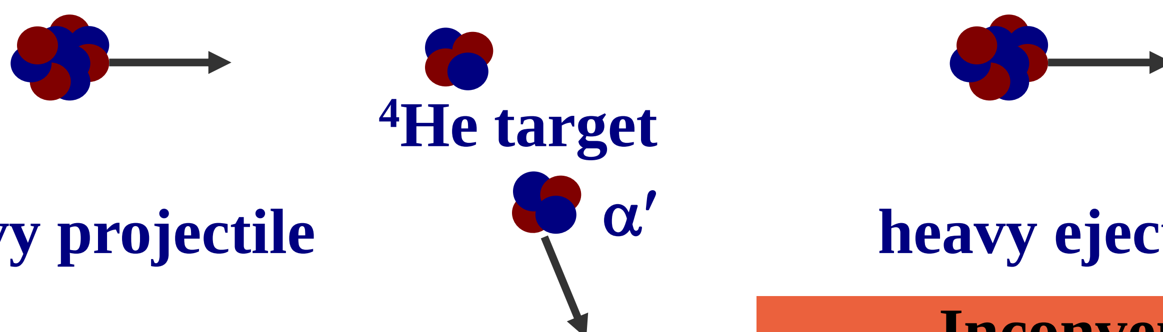

recoiling α

Inconvenience:
difficulty to detect the low-energy alphas

Storage Ring

Experimental storage ring at GSI
Luminosity: $10^{26} - 10^{27}$ cm^{-2}s^{-1}

EPJ Web of Conferences 66, 03093 (2014)

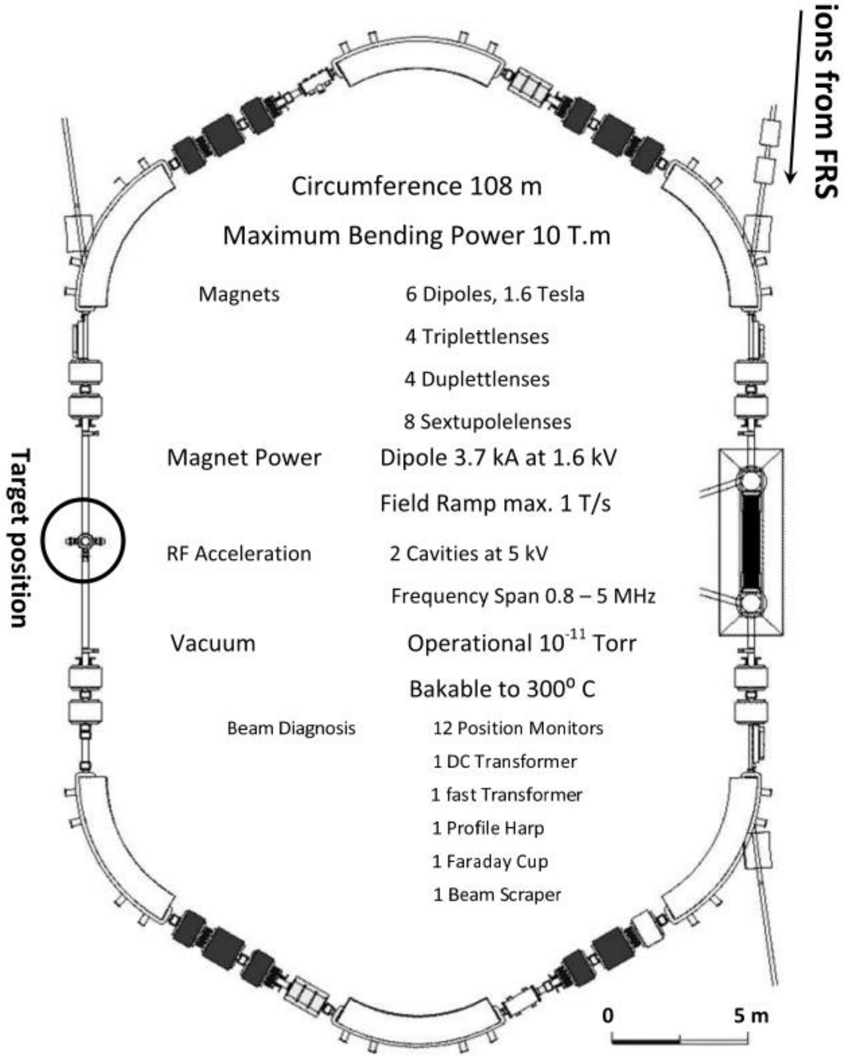

Detection system @ FAIR

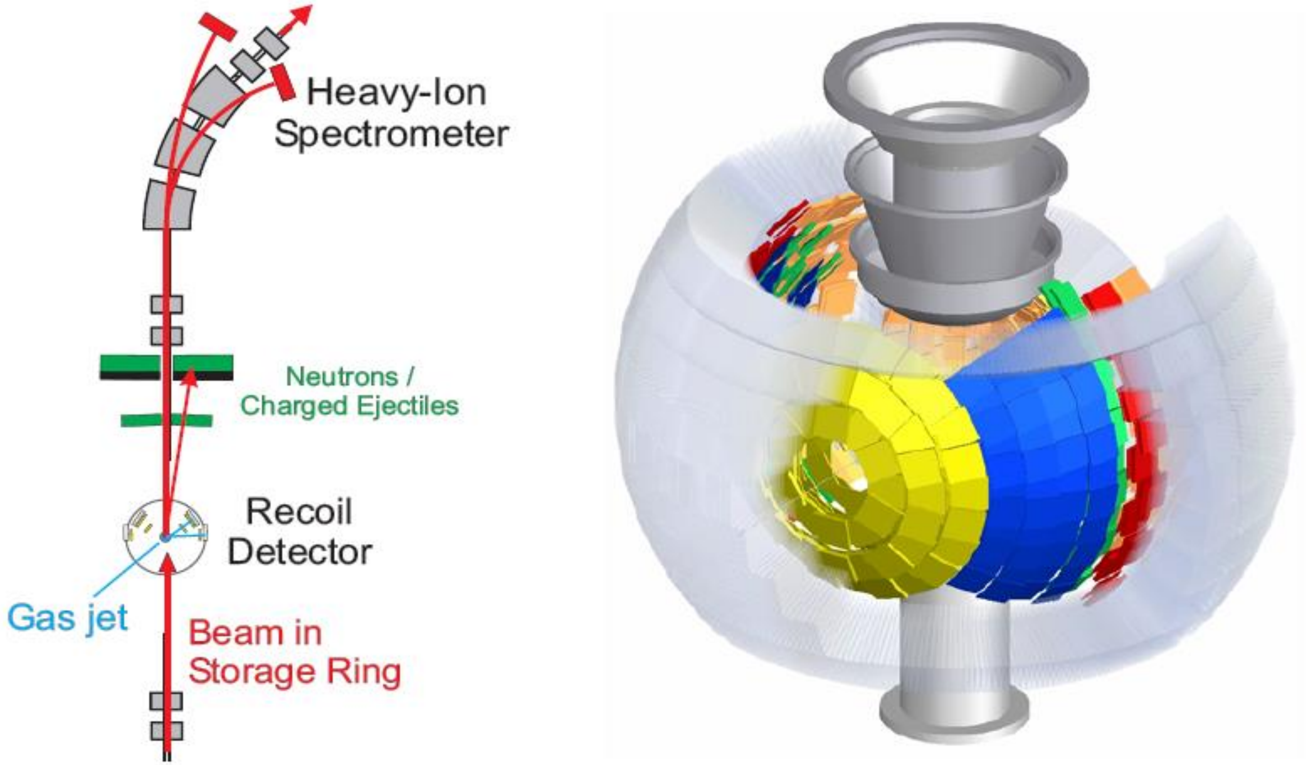

Figure 1: *Schematic view of the EXL detection systems. Left: Set-up built into the NESR storage ring. Right: Target-recoil detector surrounding the gas-jet target.*

EXL recoil prototype detector has been commissioned

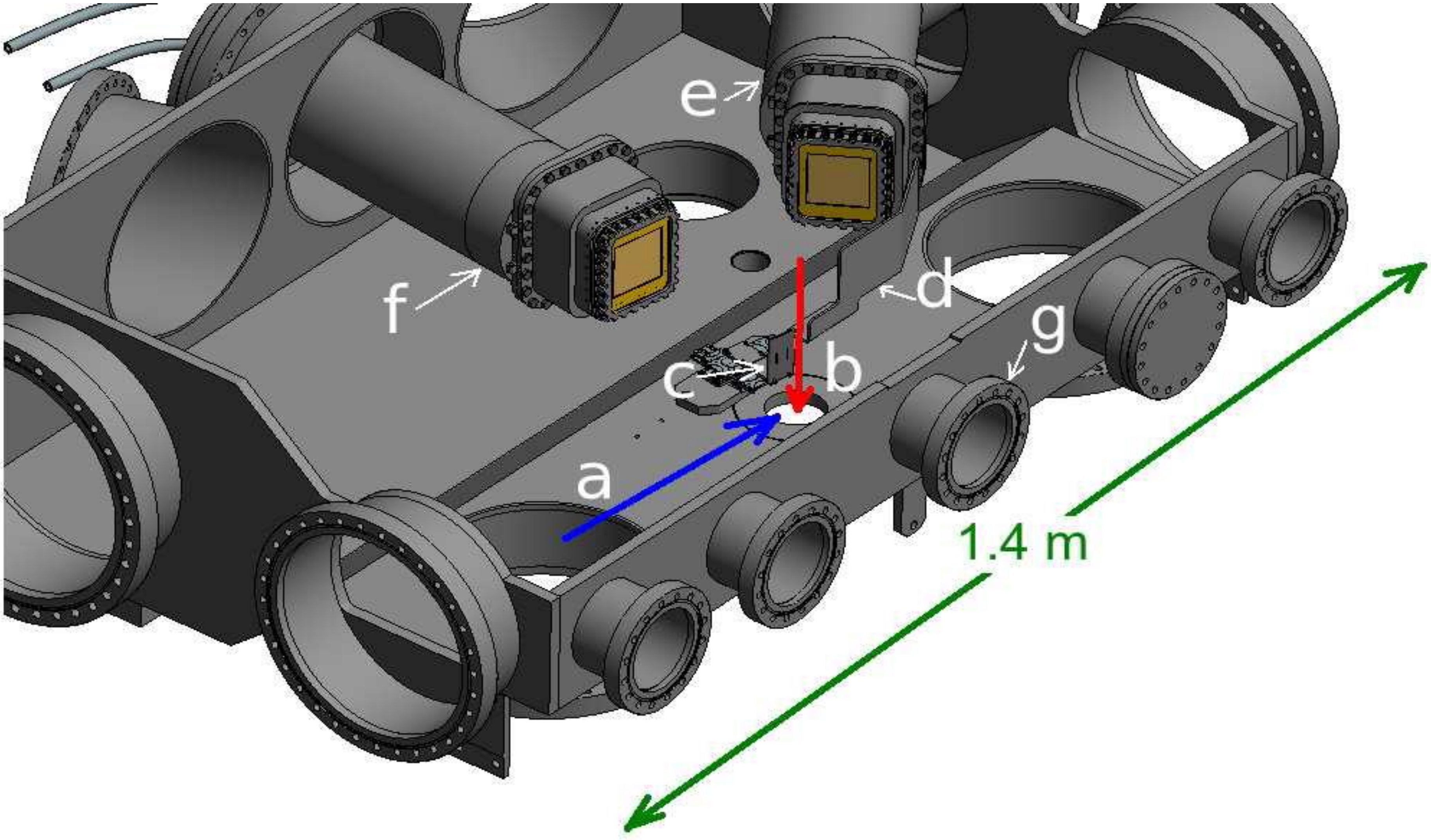
e
f
d
g
c
b
a
1.4 m

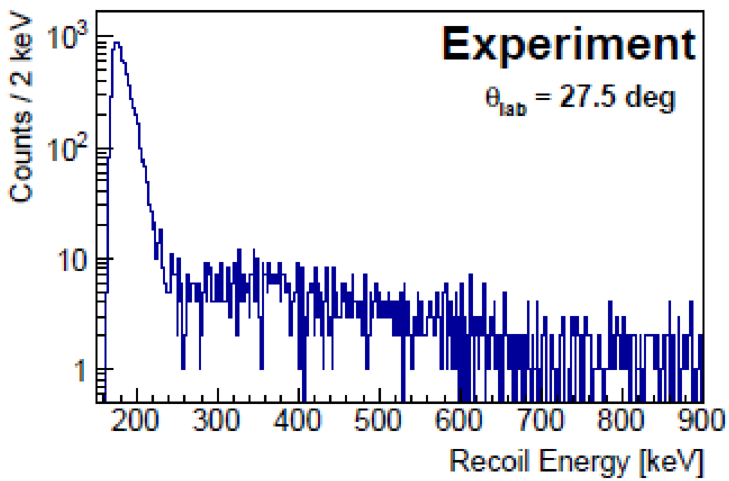

(a) Experiment, strip number 0

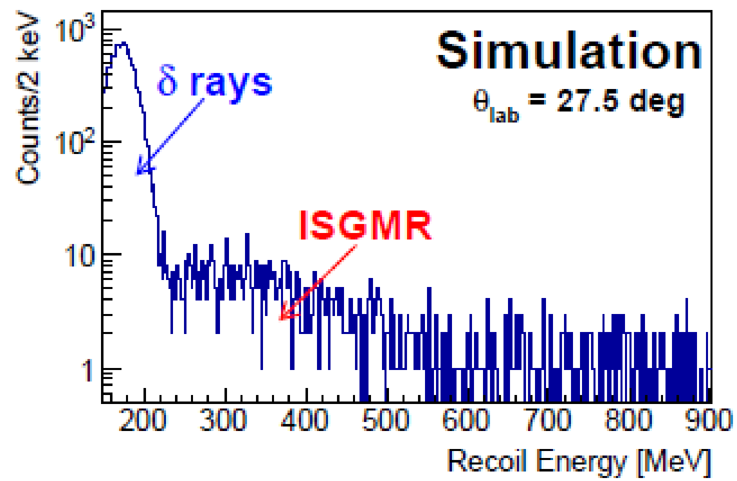

(b) Simulation, strip number 0.

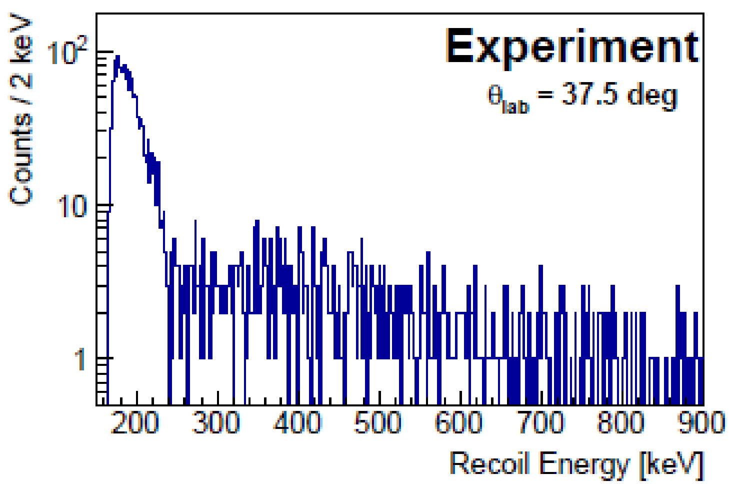

(c) Experiment, strip number 31

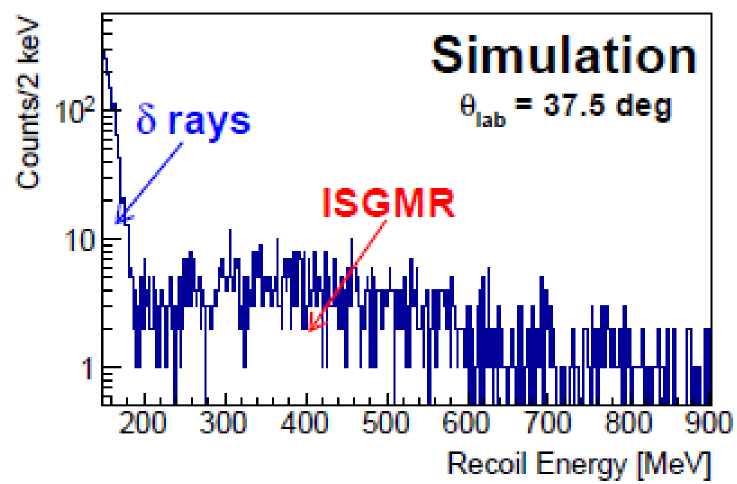

(d) Simulation, strip number 31

Active target

A gas detector where the target gas also acts as a detector

- **Good angular coverage**
- **Effective target thickness can be increased without much loss of resolution**
- **Detection of very low energy recoil particle is possible**

MAYA active-target detector at GANIL

Basics of kinematics reconstruction inside MAYA

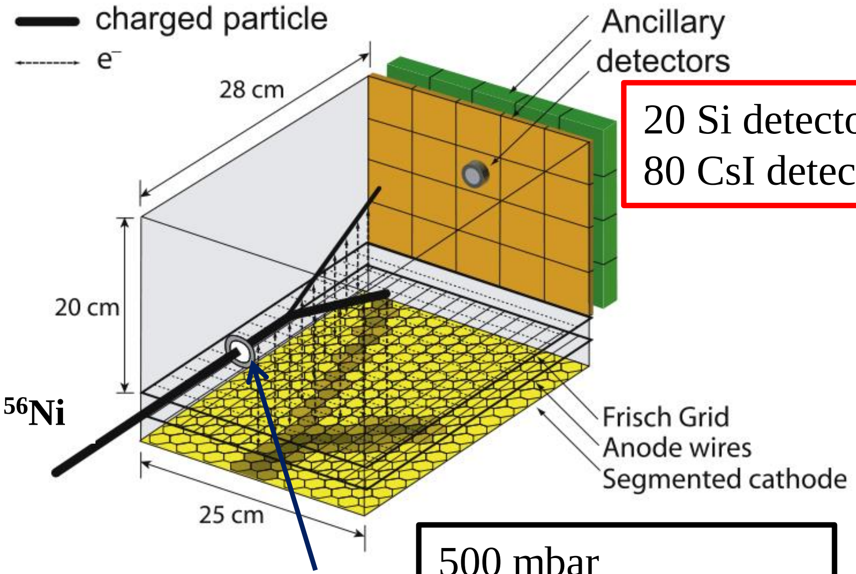

Beam ^{56}Ni

20 Si detectors
80 CsI detectors

500 mbar
95% He and 5% CF_4

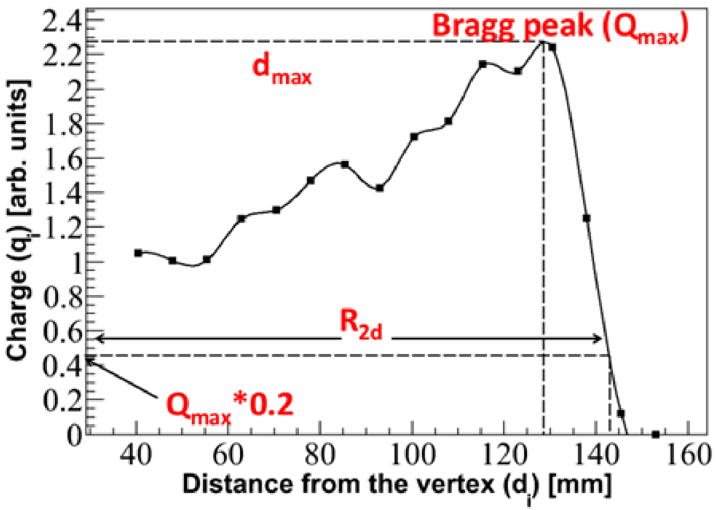

Timing information from Amplification wires

$R_{2d} \rightarrow R_{3d}$, $\theta_{2d} \rightarrow \theta_{3d}$

Range ⟶ Energy (SRIM)

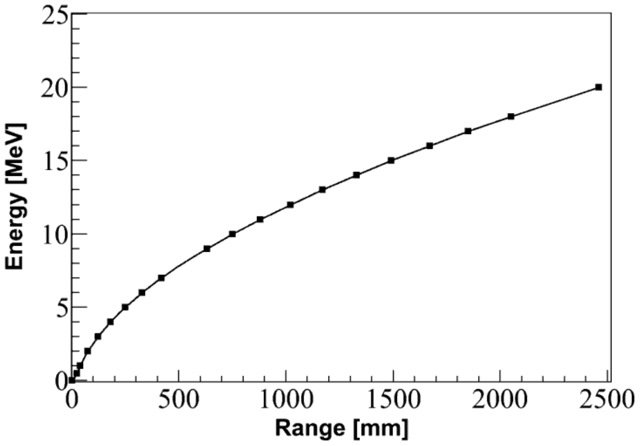

3^{rd} dimension from timing information of the anode wires

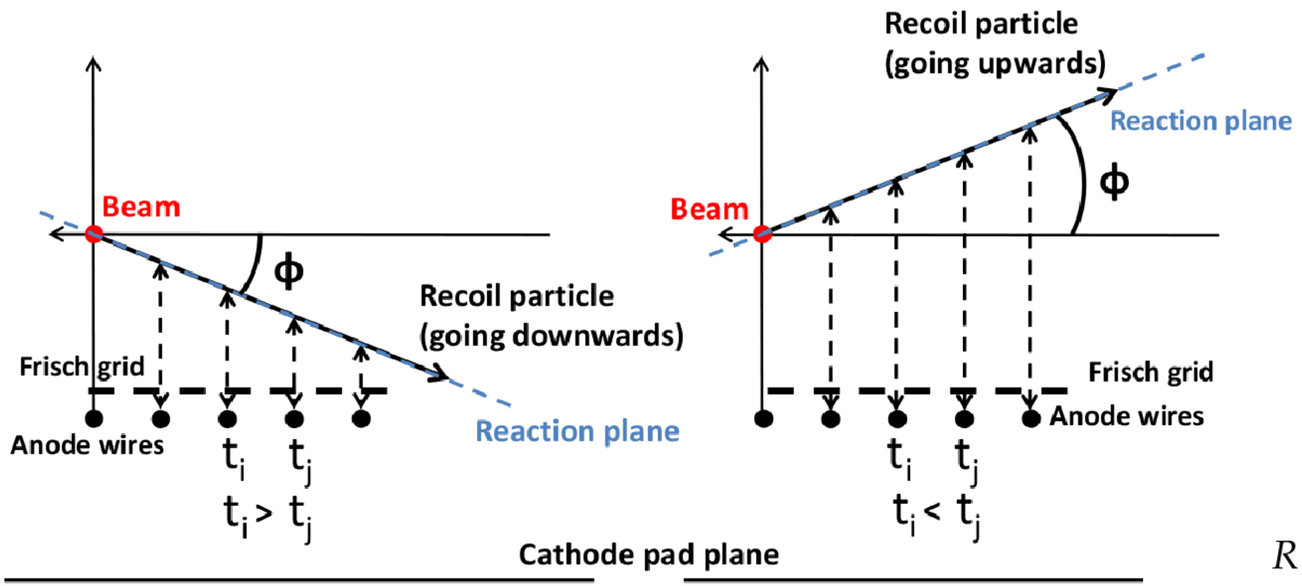

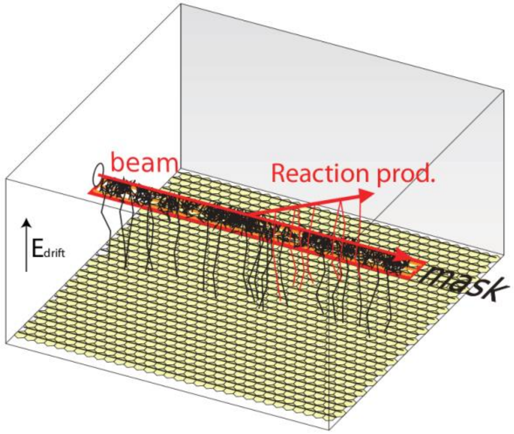

$$R = R_{2d}\sqrt{1+\sin^2\theta_{2d}\tan^2\phi}$$

Range → Energy

$$\cos\theta = \frac{\cos\theta_{2d}}{\sqrt{1+\sin^2\theta_{2d}\tan^2\phi}}$$

Kinematics plot

$^{56}Ni(\alpha,\alpha')^{56}Ni^*$

Data

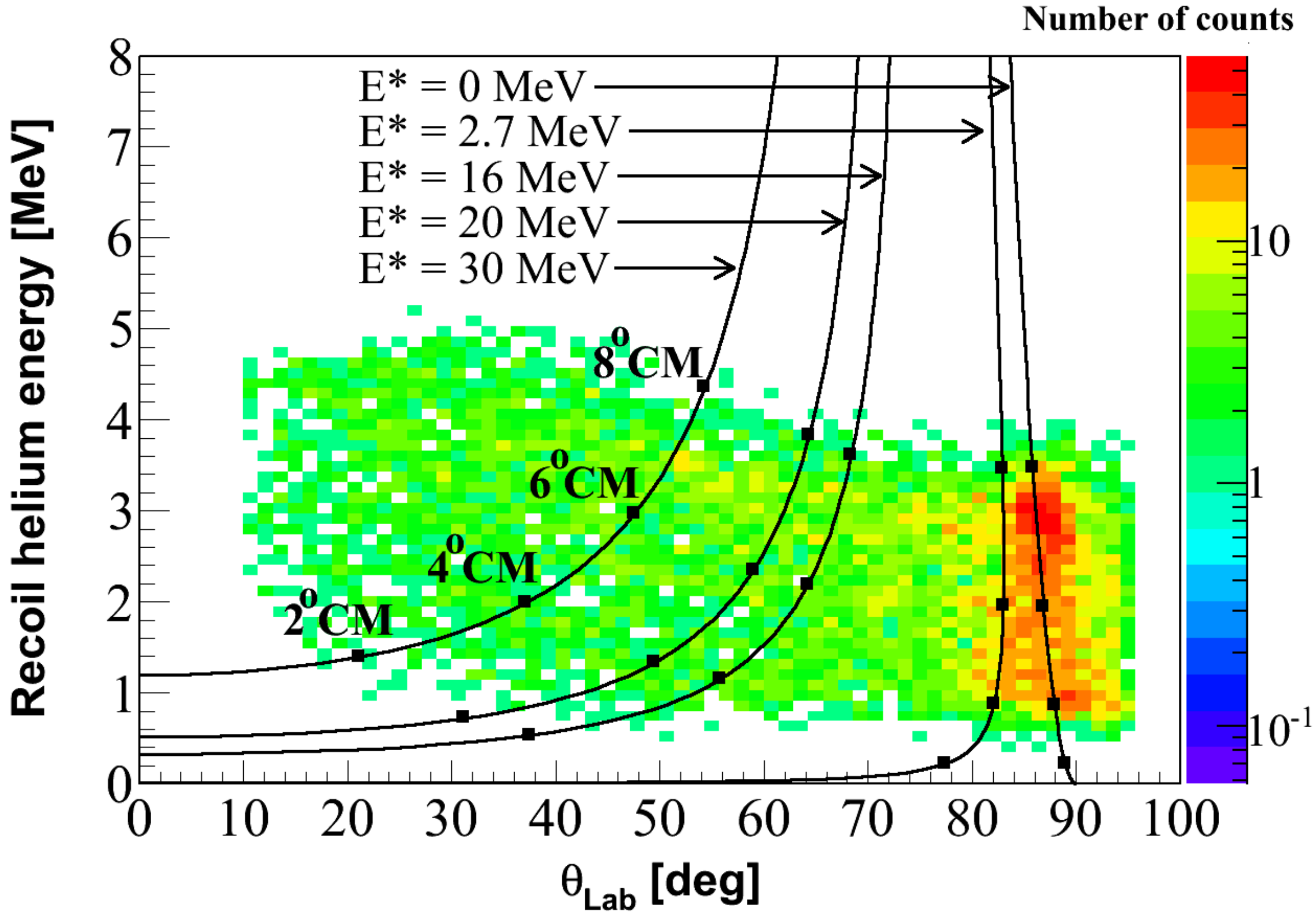

Peak fitting method

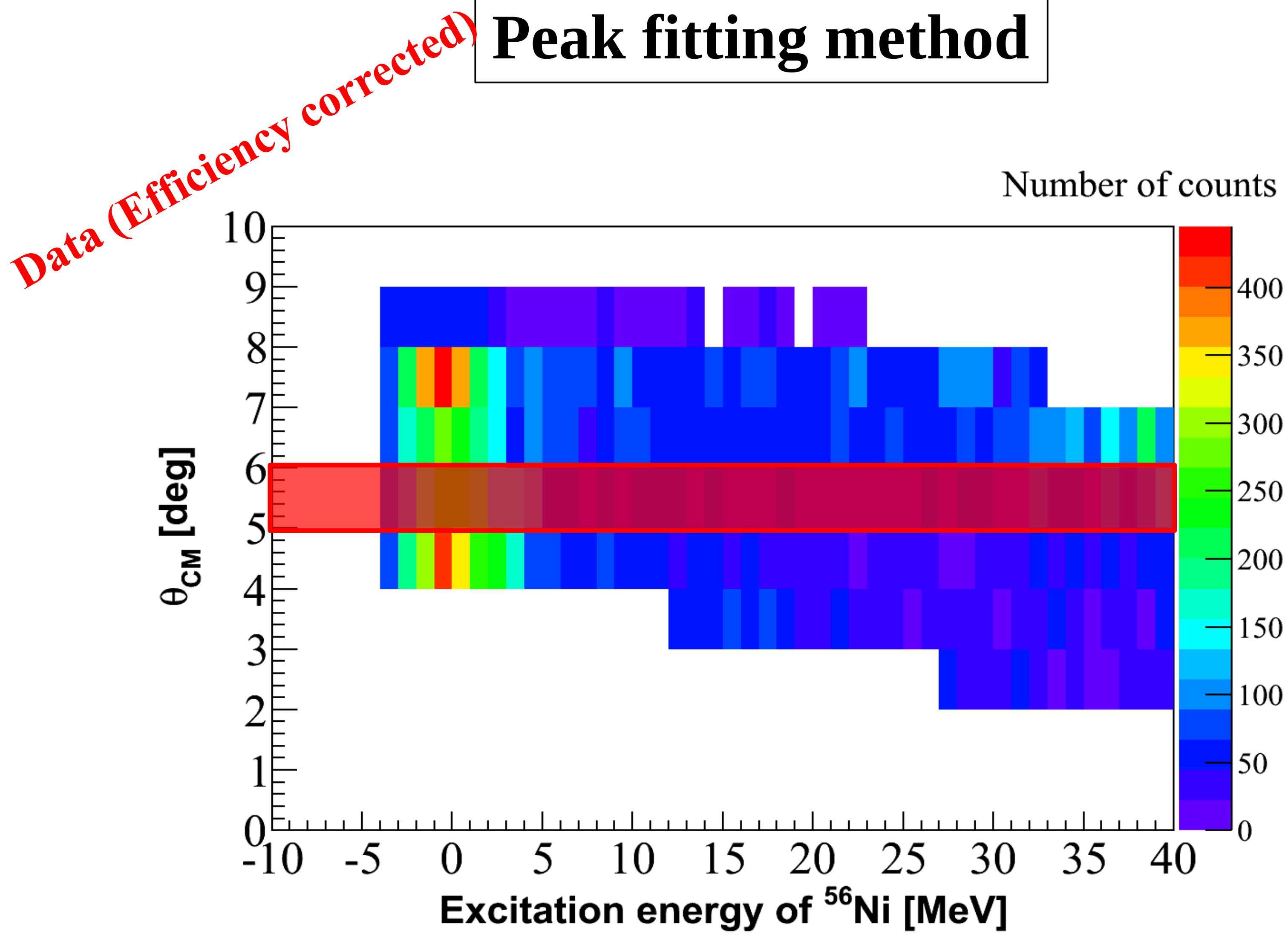

Participants

ATOMKI

- M. Csatlós
- L. Csige
- J. Gulyás
- A. Krasznahorkay
- D. Sohler

KVI

- A.M. van den Berg
- M.N. Harakeh
- M. Hunyadi (Atomki)
- M.A. de Huu
- H.J. Wörtche

NDU

- U. Garg
- T. Li
- B.K. Nayak
- M. Hedden
- M. Koss
- D. Patel
- S. Zhu

WWU

- C. Bäumer
- B.C. Junk
- S. Rakers

RCNP

- H. Akimune
- H. Fujimura
- M. Fujiwara
- K. Hara
- H. Hashimoto
- M. Itoh
- T. Murakami
- K. Nakanishi
- S. Okumura
- H. Sakaguchi
- H. Takeda
- M. Uchida
- Y. Yasuda
- M. Yosoi

E605: ISGDR in ^{56}Ni

Soumya Bagchi
Marine Vandebrouck

EXL Collaboration

Juan Carlos Zamora

M. Vandebrouck *et al*., Phys. Rev. Lett. 113 (2014) 032504
M. Vandebrouck *et al*., Phys. Rev. C 92 (2015) 024316
S. Bagchi *et al*., Phys. Lett. B751 (2015) 371

Thank you for your attention

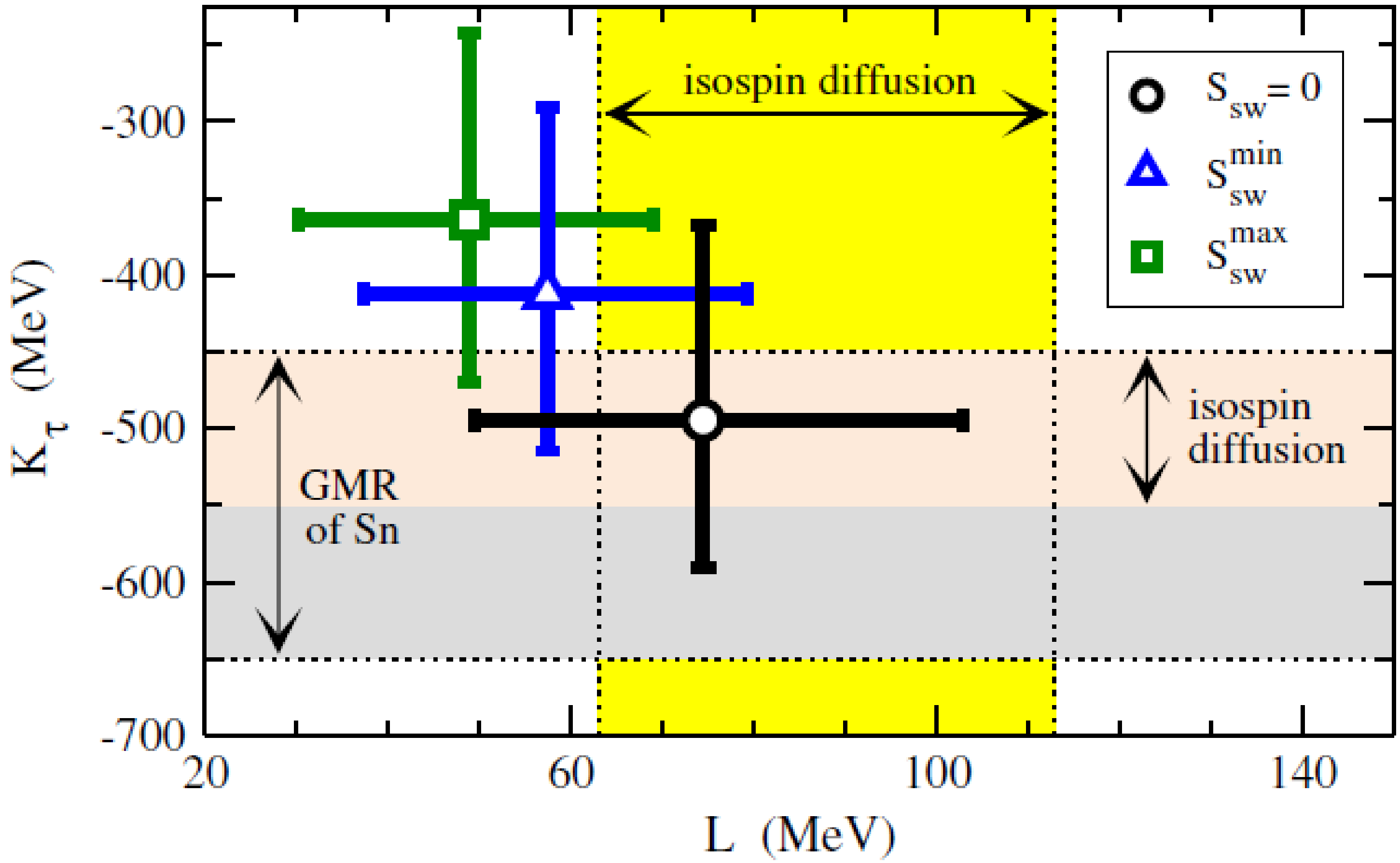

$\Rightarrow K_t = -500\ ^{+125}_{-100}$ **MeV**

M. Centelles *et al*., Phys. Rev. Lett. 102, 122502 (2009)

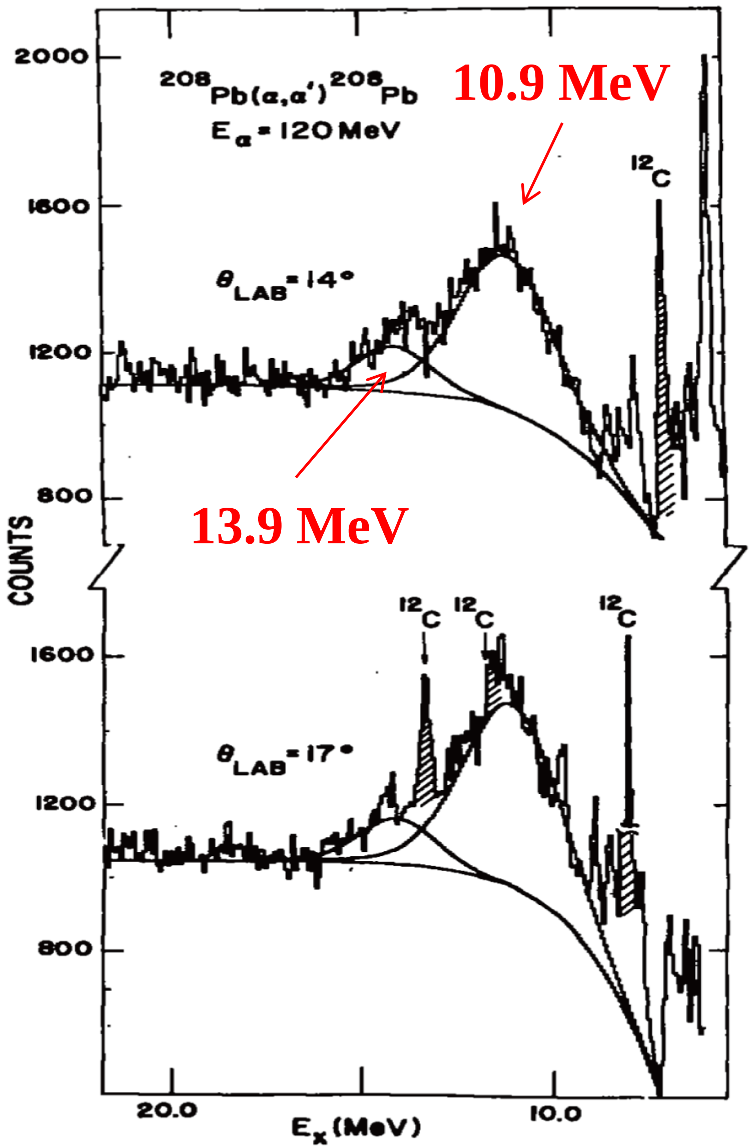

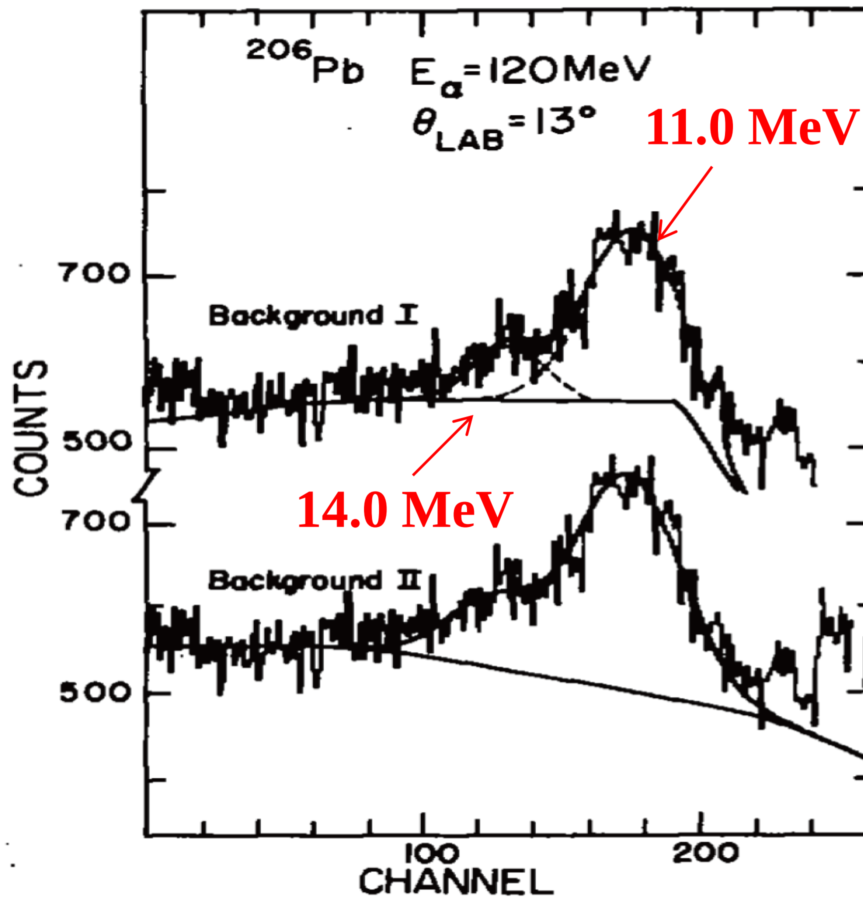

M.N. Harakeh *et al.*, Nucl. Phys. A327, 373 (1979)

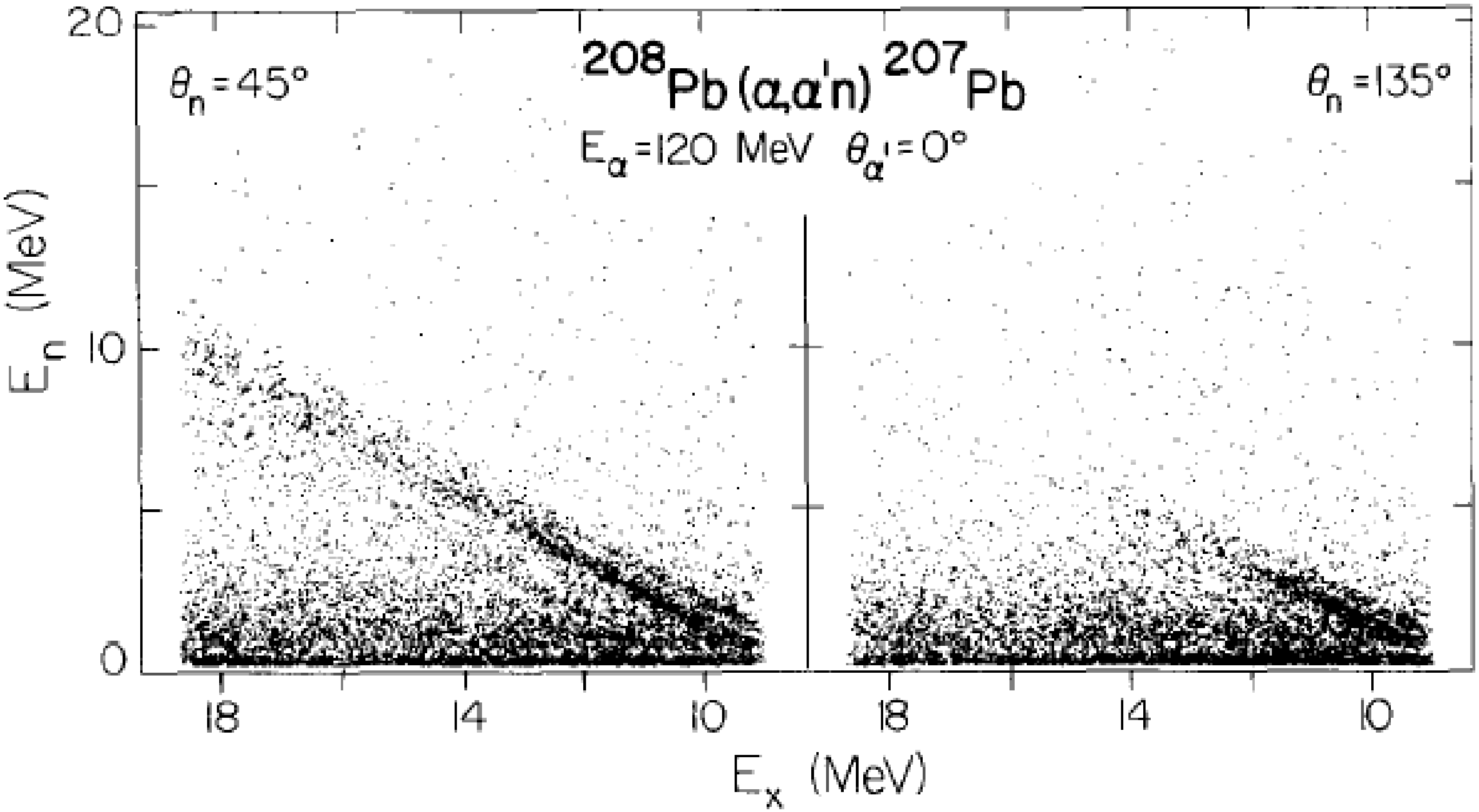

S. Brandenburg *et al*., Nucl. Phys. A466 (1987) 29

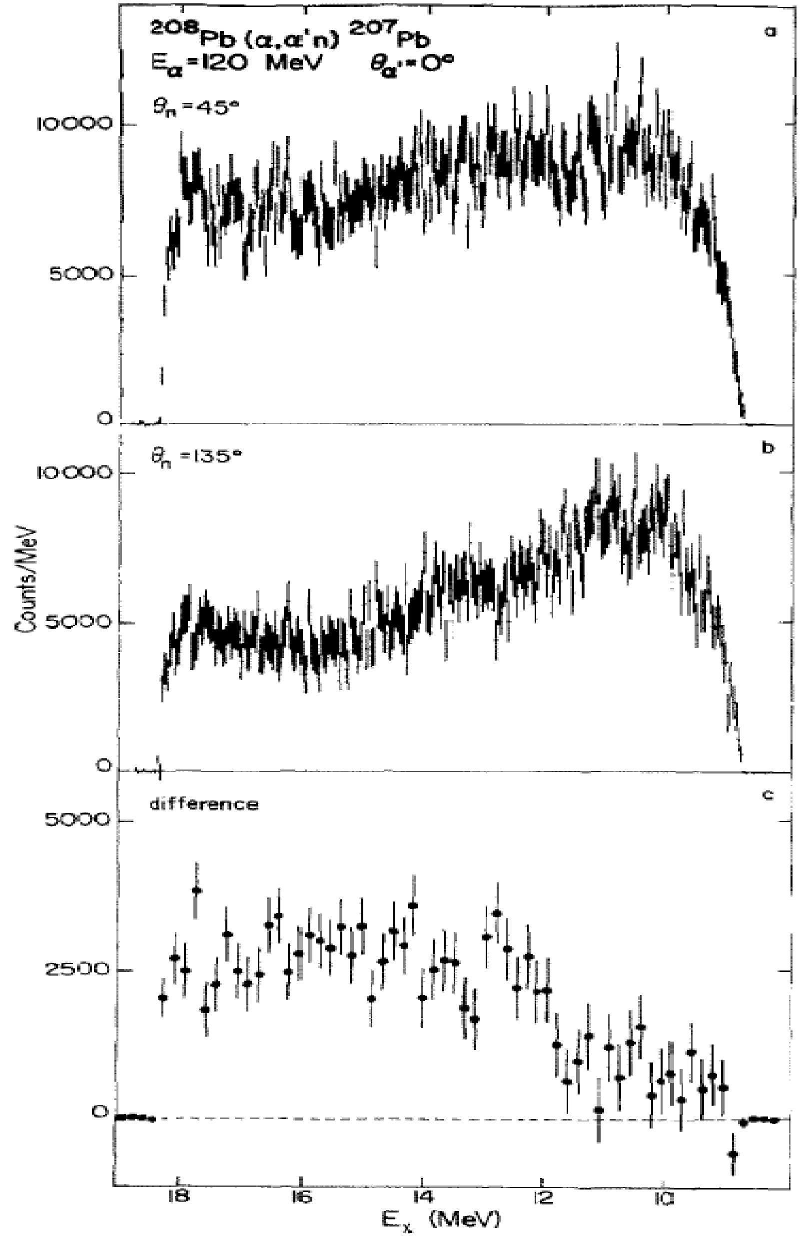

S. Brandenburg *et al.*,
Nucl. Phys. A466 (1987) 29

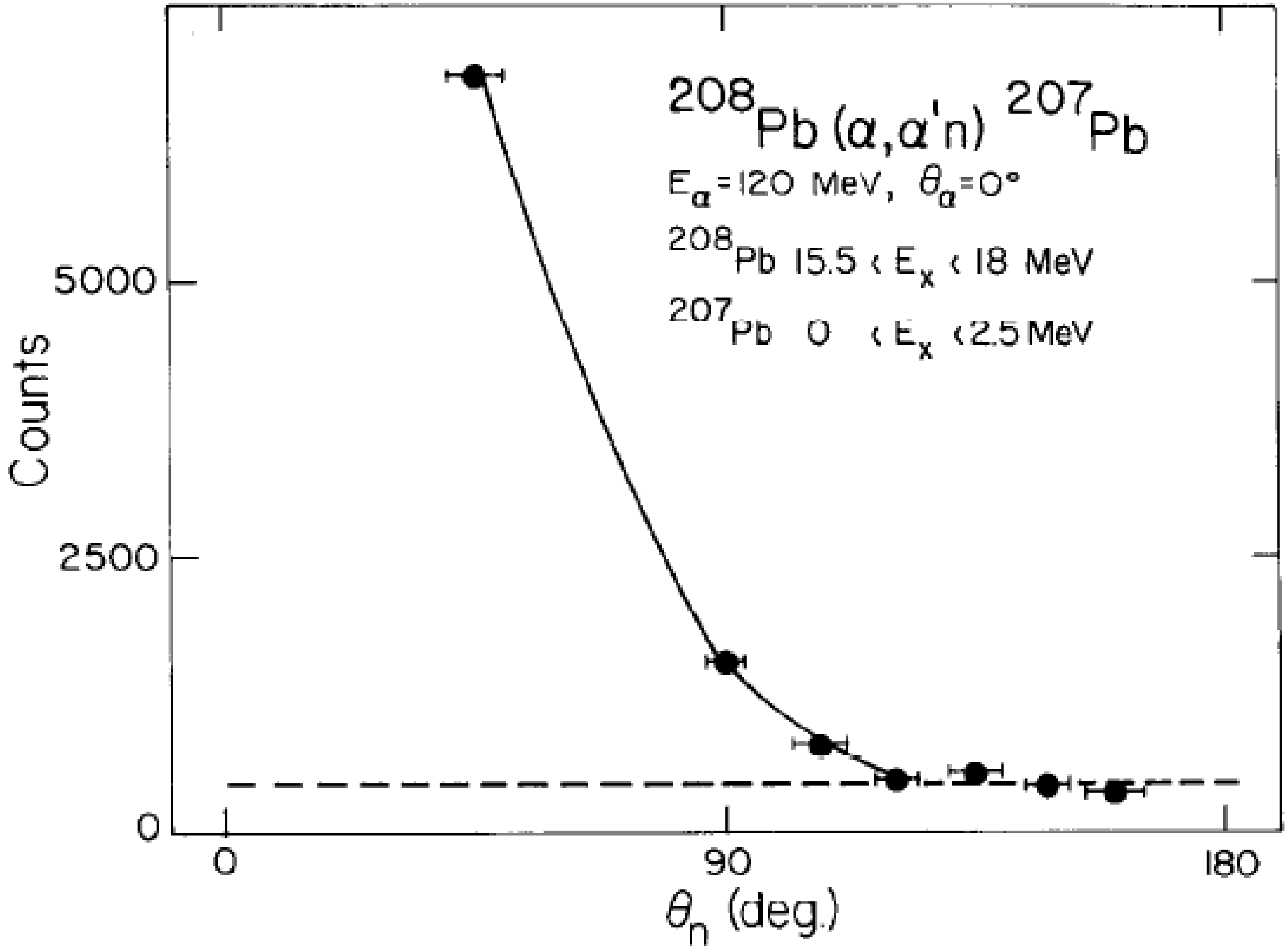

S. Brandenburg *et al.*, Nucl. Phys. A466 (1987) 29

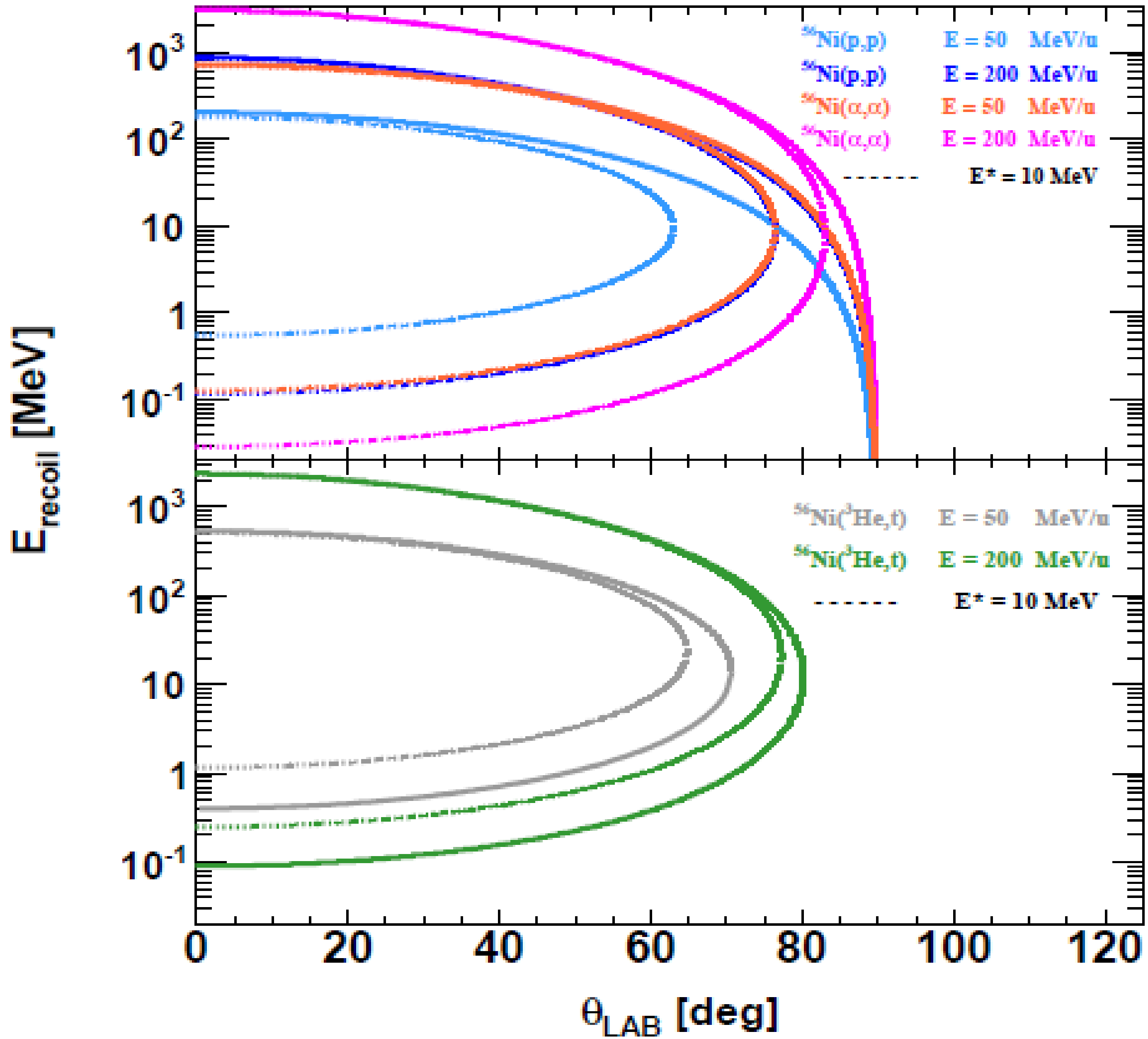

56Ni(p,p) E = 50 MeV/u
56Ni(p,p) E = 200 MeV/u
56Ni(α,α) E = 50 MeV/u
56Ni(α,α) E = 200 MeV/u
E* = 10 MeV
56Ni(3He,t) E = 50 MeV/u
56Ni(3He,t) E = 200 MeV/u
E* = 10 MeV
E_recoil [MeV]
θ_LAB [deg]

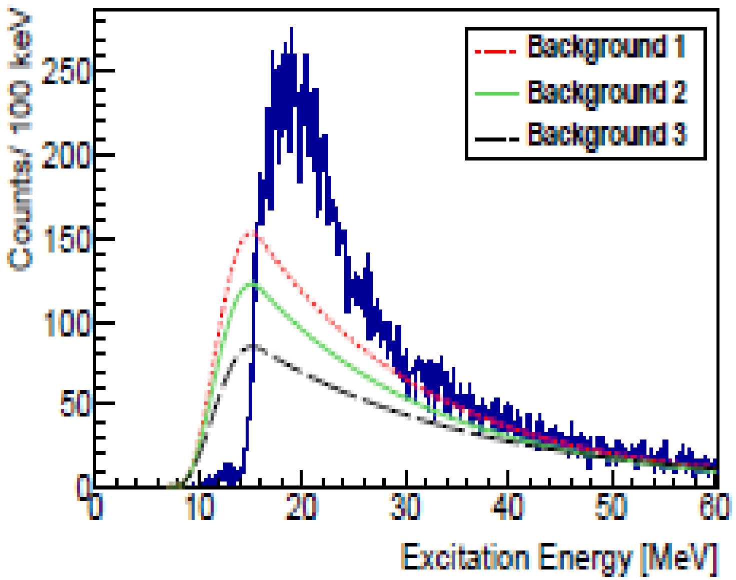

(a) The three different backgrounds studied.

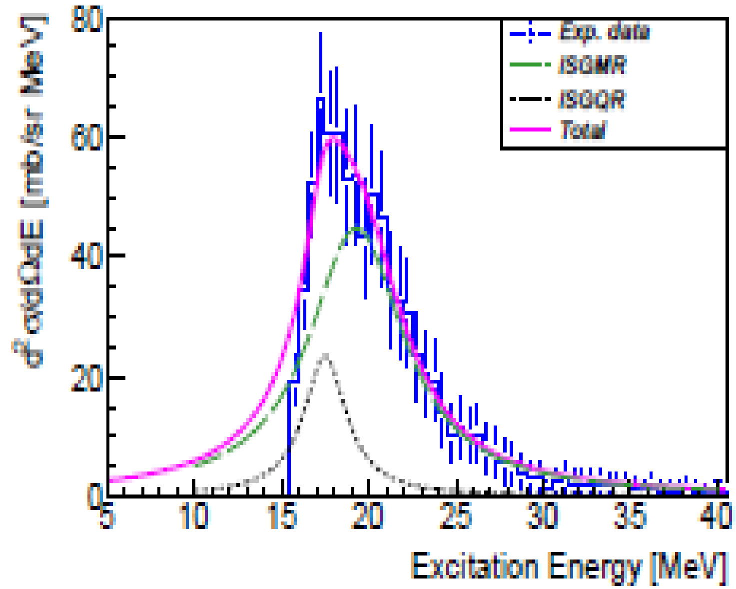

(b) Double-differential cross section after the background 2 subtraction.

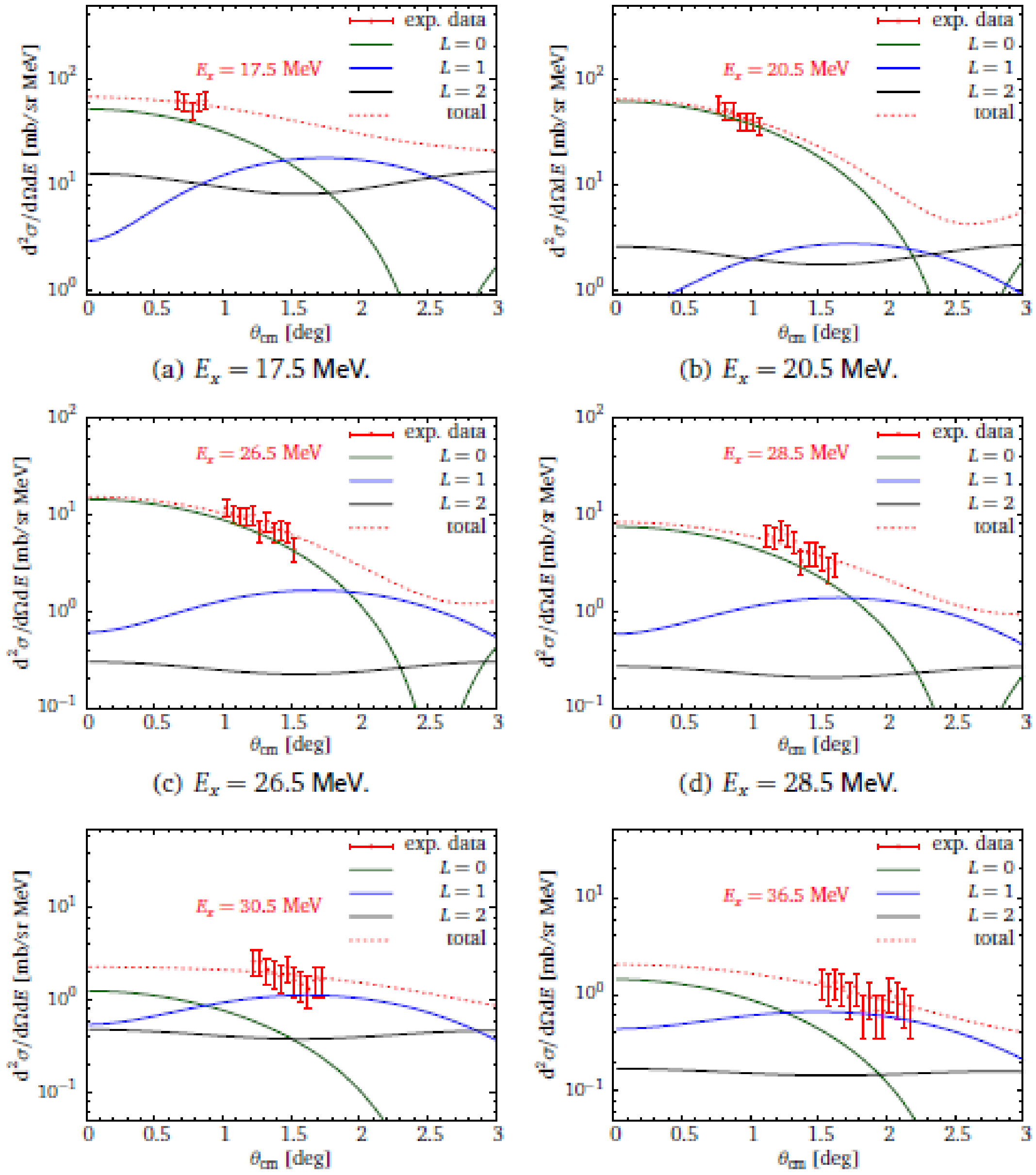

(a) $E_x = 17.5$ MeV.

(b) $E_x = 20.5$ MeV.

(c) $E_x = 26.5$ MeV.

(d) $E_x = 28.5$ MeV.

(e) $E_x = 30.5$ MeV.

(f) $E_x = 36.5$ MeV.

Excitation energy of ^{56}Ni

Data (Not efficiency corrected)

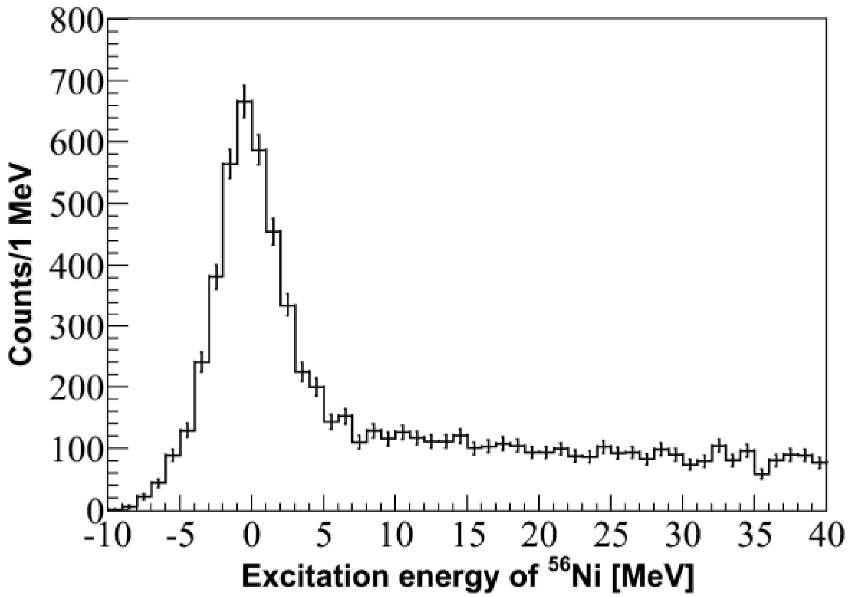

Data (Efficiency corrected)

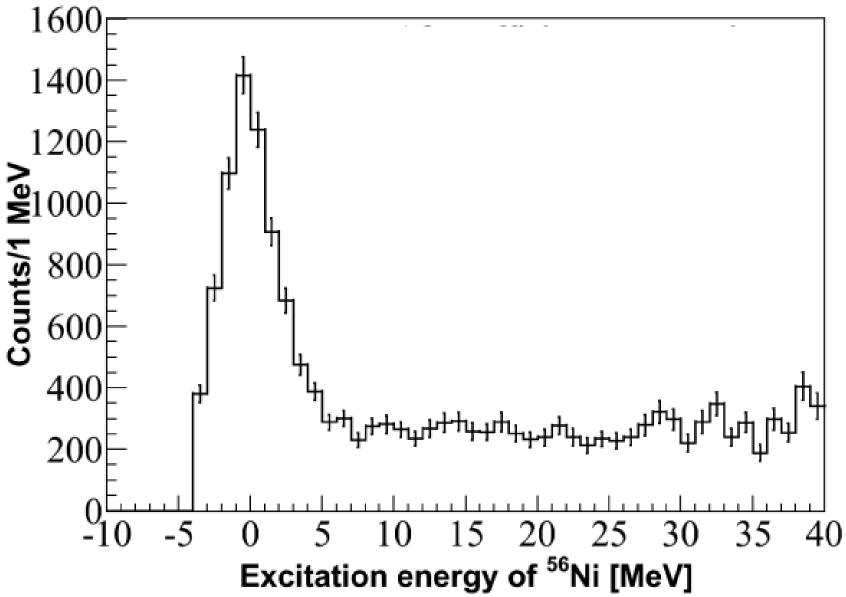

Peak fitting method

Background shape fixed manually (Background 1)

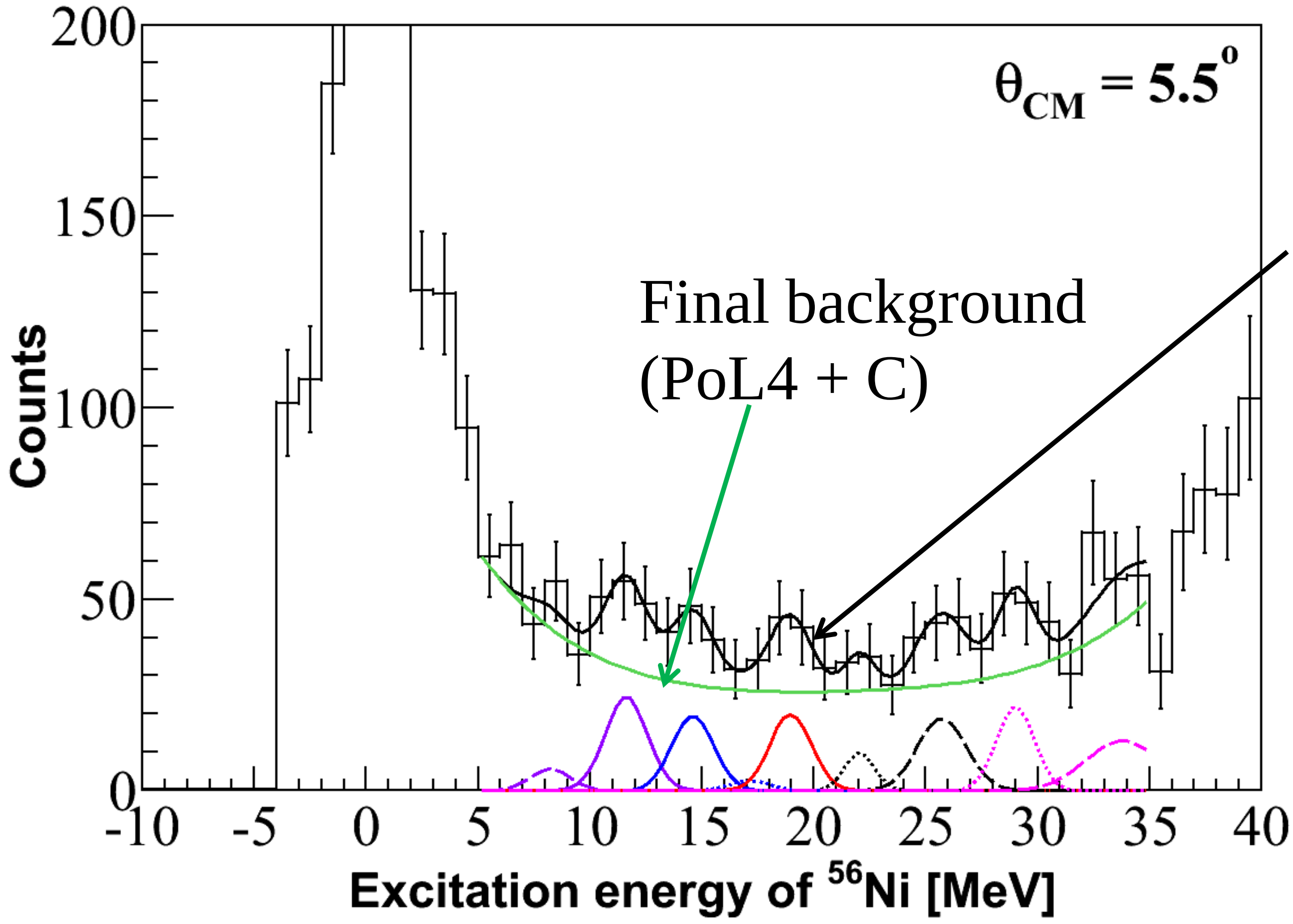

Total fit = 9 Gaussian Func. + PoL4 + C

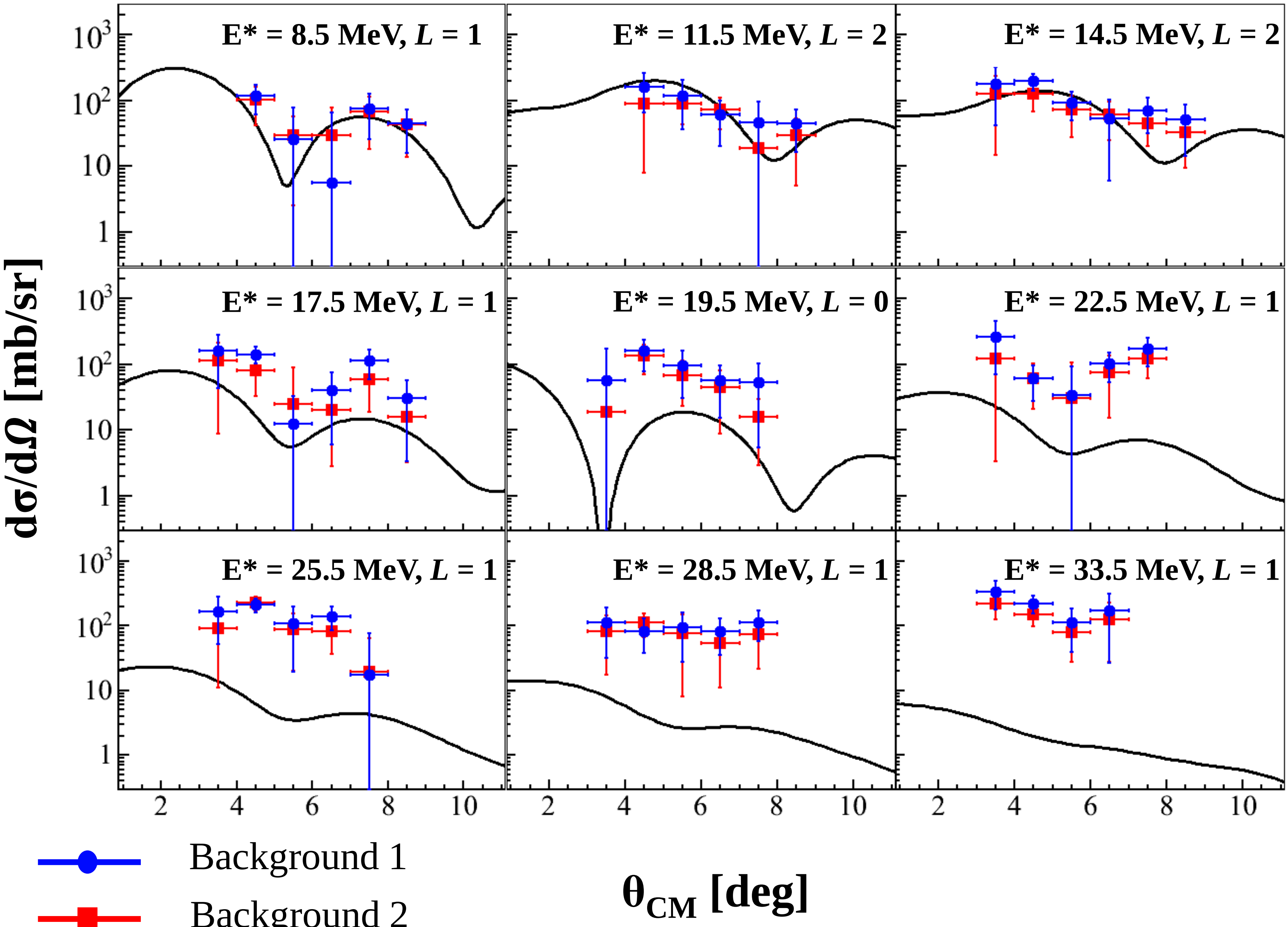
E* = 8.5 MeV, L = 1
E* = 11.5 MeV, L = 2
E* = 14.5 MeV, L = 2
E* = 17.5 MeV, L = 1
E* = 19.5 MeV, L = 0
E* = 22.5 MeV, L = 1
E* = 25.5 MeV, L = 1
E* = 28.5 MeV, L = 1
E* = 33.5 MeV, L = 1
dσ/dΩ [mb/sr]
θCM [deg]
Background 1
Background 2